Electronic Companions for Split Liver Transplantation: An Analytical Decision Support Model

Yanhan (Savannah) Tang, Alan Scheller-Wolf, Sridhar Tayur, Emily R. Perito, John P. Roberts

EC.1. Proofs for Analytical Results in Section 4

EC.1.1. Proof of Proposition 1

PROPOSITION 1. *In the interior case, the optimal decision at any $t \in \mathcal{T}$ in the optimal solution to the fluid optimization problem* (1) $\sim$ (6) *is equivalent to the solution to the following LP:*

$$\max_{(\mathbf{U}(t),\mathbf{S}(t))} \mathscr{U}_t^{NPDWT} := \mathbf{d}^\top \left\{ \int_t^T \exp[(\tau - t)\mathbf{\Psi}]\,\mathrm{d}\tau \right\} \left(\sum_\ell \mathbf{P}^\ell \mathbf{u}^\ell(t) + \bar{\mathbf{P}}^\ell \mathbf{s}^\ell(t) \right) \tag{EC.1}$$

$$s.t.\ (3) \sim (5), (18) \tag{EC.2}$$

The optimal allocation policy with the pure objective of minimizing queueing deaths solves (EC.1) $\sim$ (EC.2) *for each $t \in \mathcal{T}$ and $\ell \in \mathcal{L}$. $\mathscr{U}_t^{NPDWT}(\mathbf{U}(t), \mathbf{S}(t))$ represents the utility of the current decision $(\mathbf{U}(t), \mathbf{S}(t))$ on reducing patient deaths from now on to the end of horizon.*

In other words, we allocate livers as much as possible (subject to constraints) to the patient groups with the largest dynamic index(es) specified by the objective function.

Proof: (a) Plugging in the explicit expressions for the fluid limit vector $\mathbf{x}$ (13) $\sim$ (14):

$$\min_{(\mathbf{U},\mathbf{S})} \int_{\tau=0}^T \mathbf{d}^\top \exp[\tau\mathbf{\Psi}]\mathbf{x}(0) d\tau + \int_{\tau=0}^T \mathbf{d}^\top \int_0^\tau \exp[(\tau - t)\mathbf{\Psi}] \left(\lambda(t) - \sum_\ell \mathbf{P}^\ell \mathbf{u}^\ell(t) - \bar{\mathbf{P}}^\ell \mathbf{s}^\ell(t) \right) \mathrm{d}t\,\mathrm{d}\tau \tag{EC.3}$$

this objective written in the vector form is equivalent to

$$\begin{aligned}
&\min_{(\mathbf{U},\mathbf{S})} \int_{\tau=0}^T \sum_{i,j,i',j'} d_{ij} \left(\exp[\tau\mathbf{\Psi}]\right)_{ij,i'j'} x_{i'j'}(0)\,\mathrm{d}\tau \qquad \text{(EC.4)}\\
&+ \int_{\tau=0}^T \sum_{i,j} d_{ij} \sum_{i',j'} \int_0^\tau \left(\exp[(\tau - t)\mathbf{\Psi}]\right)_{ij,i'j'} \lambda_{i'j'}(t)\,\mathrm{d}t\,\mathrm{d}\tau\\
&- \int_{\tau=0}^T \sum_{i,j} d_{ij} \sum_{i',j'} \int_0^\tau \left(\exp[(\tau - t)\mathbf{\Psi}]\right)_{ij,i'j'} \left(\sum_\ell P^\ell_{i'j'} u^\ell_{i'j'}(t) \right.\\
&\qquad \left. + \sum_{i'',j''} \bar{P}^\ell_{i'j',(i'j',i''j'')} s^\ell_{i'j',i''j''}(t) + \bar{P}^\ell_{i'j',(i''j'',i'j')} s^\ell_{i''j'',i'j'}(t) \right) \mathrm{d}t\,\mathrm{d}\tau.
\end{aligned}$$

Dropping the constants, it can be further simplified to

$$\begin{aligned}
&\min_{(\mathbf{U},\mathbf{S})} \int_{\tau=0}^T \sum_{i,j} d_{ij} \sum_{i',j'} \int_0^\tau \left(\exp[(\tau - t)\mathbf{\Psi}]\right)_{ij,i'j'} \left(- \sum_\ell P^\ell_{i'j'} u^\ell_{i'j'}(t) \right.\\
&\qquad \left. - \sum_{i'',j''} \bar{P}^\ell_{i'j',(i'j',i''j'')} s^\ell_{i'j',i''j''}(t) - \bar{P}^\ell_{i'j',(i''j'',i'j')} s^\ell_{i''j'',i'j'}(t) \right) \mathrm{d}t\,\mathrm{d}\tau.
\end{aligned}$$

Recall that in the interior case patient buffers are always non-empty. Thus, decisions decompose, and the expression above can be further decomposed into

$$\max_{(\mathbf{U},\mathbf{S})} \int_{\tau=0}^{T} \sum_{i,j} d_{ij} \sum_{i',j'} \int_0^{\tau} \left(\exp[(\tau-t)\mathbf{\Psi}]\right)_{ij,i'j'} \Bigg(\sum_{\ell} P^{\ell}_{i'j'} u^{\ell}_{i'j'}(t) + \sum_{i'',j''} \bar{P}^{\ell}_{i'j',(i'j',i''j'')} s^{\ell}_{i'j',i''j''}(t) + \bar{P}^{\ell}_{i'j',(i''j'',i'j')} s^{\ell}_{i''j'',i'j'}(t) \Bigg) \mathrm{d}t\, \mathrm{d}\tau.$$

Now, we use a transformation to obtain a simple, myopic objective. More specifically, we look at the decision rule at each $t \in [0,T]$: Note that integration and summation can be exchanged in the formula above, and the term to be integrated, $g_{\ell,ij,i'j'}(\tau,t) := \sum_{i,j} d_{ij} \sum_{i',j'} \left(\exp[(\tau-t)\mathbf{\Psi}]\right)_{ij,i'j'} \left(\sum_{\ell} P^{\ell}_{i'j'} u^{\ell}_{i'j'}(t) + \sum_{i'',j''} \bar{P}^{\ell}_{i'j',(i'j',i''j'')} s^{\ell}_{i'j',i''j''}(t) + \bar{P}^{\ell}_{i'j',(i''j'',i'j')} s^{\ell}_{i''j'',i'j'}(t) \right)$ appears for all $T \geq \tau \geq t$, but not for $0 \leq \tau \leq t$; therefore,

$$\int_{\tau=0}^{T} \int_{t=0}^{\tau} g_{\ell,ij,i'j'}(\tau,t)\, \mathrm{d}t\, \mathrm{d}\tau = \int_{t=0}^{T} \int_{\tau=t}^{T} g_{\ell,ij,i'j'}(\tau,t)\, \mathrm{d}\tau\, \mathrm{d}t. \tag{EC.5}$$

Note that the RHS of (EC.5) is an integration over decisions at t for all $t \in \mathcal{T}$, and the expected influences of all decisions are fully extracted (looking forward), thus we do not see carry-over effects (we only have u and s variables in the expression); whereas in the original objective function (1), x appears and thus we couldn't decompose decision rules for each time t. Furthermore, because of the way we characterize capacity constraints ((4) $\sim$ (5)) in the fluid approximation, decisions at time t to optimize over $\int_{\tau=t}^{T} g_{\ell,ij,i'j'}(\tau,t)\, \mathrm{d}\tau$ are independent. This is reasonable because in general livers deteriorate quickly, and they are allocated as soon as they become available. In other words, we extract the exact expected "impact" or influence of our decision at time t explicitly, and we can then solve the fluid optimal policy by directly optimizing over this impact at each time t:

$$\max_{(\mathbf{U}(t),\mathbf{S}(t))} \sum_{i,j} d_{ij} \sum_{i'j'} \left\{ \int_t^T \left(\exp[(\tau-t)\mathbf{\Psi}]\right)_{ij,i'j'} \mathrm{d}\tau \right\} \Bigg(\sum_{\ell} P^{\ell}_{i'j'} u^{\ell}_{i'j'}(t) + \sum_{i'',j''} \bar{P}^{\ell}_{i'j',(i'j',i''j'')} s^{\ell}_{i'j',i''j''}(t) + \bar{P}^{\ell}_{i'j',(i''j'',i'j')} s^{\ell}_{i''j'',i'j'}(t) \Bigg) \tag{EC.6}$$

Writing (EC.6) in vector form we arrive at (EC.1). *Q.E.D.*

EC.1.2. Proof of Proposition 2

Proposition 2. *The fluid optimization problem* (7) $\sim$ (8) *can be decomposed into the following optimization problem:*

$$\begin{aligned} \max_{\mathbf{U}(t),\mathbf{S}(t)} \quad & \mathscr{U}_t^{QALY} := -\sum_{\ell} \mathbf{q}^{\top} \left\{ \int_t^T \exp[(\tau-t)\mathbf{\Psi}]\, \mathrm{d}\tau \right\} \left(\mathbf{P}^{\ell}\mathbf{u}^{\ell}(t) + \bar{\mathbf{P}}^{\ell}\mathbf{s}^{\ell}(t) \right) \\ & \qquad + \mathbf{H}^{\ell}\mathbf{P}^{\ell}\mathbf{u}^{\ell}(t) + \bar{\mathbf{H}}^{\ell}\bar{\mathbf{P}}^{\ell}\mathbf{s}^{\ell}(t) \\ s.t. \quad & (3) \sim (5), (18) \end{aligned}$$

In the interior case, the optimal allocation policy with the objective to maximize QALY solves (19) $\sim$ (20).

Proof: The maximizing QALY objective (8) is:

$$\begin{aligned}\max_{(\mathbf{U},\mathbf{S})} \quad & \text{OBJ}^{\text{QALY}} := \int_0^T \left\{ \mathbf{q}^\top \mathbf{x}(t) + \sum_\ell \mathbf{H}^\ell \mathbf{P}^\ell \mathbf{u}^\ell(t) + \mathbf{H}^\ell \bar{\mathbf{P}}^\ell \mathbf{s}^\ell(t) \right\} \mathrm{d}t \\ s.t. \quad & (2) \sim (6)\end{aligned}$$

The reformulation and decomposition techniques for $\int_0^T \mathbf{q}^\top \mathbf{x}(t)\,\mathrm{d}t$ is the same as those for $\int_0^T \mathbf{q}^\top \mathbf{x}(t)\,\mathrm{d}t$, following the same procedure presented in Section EC.1.1, we can decompose the cumulative queueing QALY into:

$$\begin{aligned}\max_{\mathbf{U}(t),\mathbf{S}(t)} \quad & -\sum_\ell \mathbf{q}^\top \left\{ \int_t^T \exp[(\tau - t)\mathbf{\Psi}]\,\mathrm{d}\tau \right\} \left(\mathbf{P}^\ell \mathbf{u}^\ell(t) + \bar{\mathbf{P}}^\ell \mathbf{s}^\ell(t) \right) \\ s.t. \quad & (3) \sim (5), (18)\end{aligned}$$

Note that Section EC.1.1 has a minimization objective, whereas here we are maximizing QALY, thus we put a minus sign in the objective function.

The second and third terms in the objective function, $\int_0^T \sum_\ell \mathbf{H}^\ell \mathbf{P}^\ell \mathbf{u}^\ell(t) + \mathbf{H}^\ell \bar{\mathbf{P}}^\ell \mathbf{s}^\ell(t)\,\mathrm{d}t$, can be directly decomposed into each time t. Thus, we can decompose the allocation problem with the QALY objective into:

$$\begin{aligned}\max_{\mathbf{U}(t),\mathbf{S}(t)} \quad & \mathscr{U}_t^{\text{QALY}} := -\sum_\ell \mathbf{q}^\top \left\{ \int_t^T \exp[(\tau - t)\mathbf{\Psi}]\,\mathrm{d}\tau \right\} \left(\mathbf{P}^\ell \mathbf{u}^\ell(t) + \bar{\mathbf{P}}^\ell \mathbf{s}^\ell(t) \right) \\ & \qquad + \mathbf{H}^\ell \mathbf{P}^\ell \mathbf{u}^\ell(t) + \bar{\mathbf{H}}^\ell \bar{\mathbf{P}}^\ell \mathbf{s}^\ell(t) \\ s.t. \quad & (3) \sim (5), (18)\end{aligned}$$

EC.1.3. Proof of Proposition 3

PROPOSITION 3. *When $\mathbf{\Psi}$ is non-singular, $\mathscr{U}^{NPDWT}$ and $\mathscr{U}^{QALY}$ can be simplified to*

$$\mathscr{U}_t^{NPDWT} = \mathbf{d}^\top \left(\exp((T-t)\mathbf{\Psi}) - \mathbf{I} \right) \mathbf{\Psi}^{-1} \left(\sum_\ell \mathbf{P}^\ell \mathbf{u}^\ell(t) + \bar{\mathbf{P}}^\ell \mathbf{s}^\ell(t) \right)$$

$$\mathscr{U}_t^{QALY} = -\mathbf{q}^\top \left(\exp((T-t)\mathbf{\Psi}) - \mathbf{I} \right) \mathbf{\Psi}^{-1} \left(\sum_\ell \mathbf{P}^\ell \mathbf{u}^\ell(t) + \bar{\mathbf{P}}^\ell \mathbf{s}^\ell(t) \right) + \sum_\ell \mathbf{H}^\ell \mathbf{P}^\ell \mathbf{u}^\ell(t) + \bar{\mathbf{H}}^\ell \bar{\mathbf{P}}^\ell \mathbf{s}^\ell(t)$$

Proof: When $\mathbf{\Psi}$ is non-singular, it is invertible, i.e., $\mathbf{\Psi}^{-1}$ exists. The following always holds (Van Loan 1978):

$$\int_{\tau=t}^T e^{\tau \mathbf{\Psi}}\,\mathrm{d}\tau = \left(\exp(T\mathbf{\Psi}) - \exp(t\mathbf{\Psi}) \right) \mathbf{\Psi}^{-1} \tag{EC.7}$$

Plugging (EC.7) into (EC.1) and (19) gives (21) and (22), respectively.

EC.2. Alternative Transplantation Objectives

This section presents the analytical results/formulation for three alternative transplantation objectives: minimizing the total number of patient deaths (TNPD), minimizing the number of patient deaths after transplant (NPDAT), and minimizing organ wastage (OW).

EC.2.1. TNPD and NPDAT

While we focused on NPDWT and QALY objectives in the main text, our fluid limit decomposition method can be applied to other commonly used transplantation objectives. For TNPD (9) and TNPDAT (10) objectives defined in Section 3, Proposition EC.1 presents the closed-form objective functions $\mathscr{U}^{TNPD}, \mathscr{U}^{NPDAT}$ which are parts of the decomposed LPs that give optimal decision rules, respectively.

PROPOSITION EC.1. *When $\mathbf{\Psi}$ is non-singular, $\mathscr{U}^{TNPD}$ and $\mathscr{U}^{NPDAT}$ can be simplified to*

$$\mathscr{U}_t^{TNPD} = \mathbf{d}^\top \left(\exp((T-t)\mathbf{\Psi}) - \mathbf{I}\right) \mathbf{\Psi}^{-1} \left(\sum_\ell \mathbf{P}^\ell \mathbf{u}^\ell + \bar{\mathbf{P}}^\ell \mathbf{s}^\ell \right) + \sum_\ell \boldsymbol{\zeta}^\ell \mathbf{P}^\ell \mathbf{u}^\ell + \bar{\boldsymbol{\zeta}}^\ell \bar{\mathbf{P}}^\ell \mathbf{s}^\ell \tag{EC.8}$$

$$\mathscr{U}_t^{NPDAT} = \sum_\ell \boldsymbol{\zeta}^\ell \mathbf{P}^\ell \mathbf{u}^\ell + \bar{\boldsymbol{\zeta}}^\ell \bar{\mathbf{P}}^\ell \mathbf{s}^\ell \tag{EC.9}$$

Note that $\mathscr{U}_t^{\text{TNPD}} = \mathscr{U}_t^{\text{NPDAT}} + \mathscr{U}_t^{\text{NPDWT}}$, because by definition, the total number of patient deaths equals the number of patient deaths while waiting for transplants plus the number of patient deaths during and after transplants.

EC.2.2. Minimizing Organ Wastage

Another important transplantation objective is to minimize organ wastage (OW).

$$\min_{(\mathbf{U},\mathbf{S})} \quad \text{OBJ}^{\text{OW}} := \sum_\ell \int_0^T \left(\boldsymbol{\mu}^{\boldsymbol{\ell}}(\boldsymbol{t}) - \mathbf{1}_{I\cdot J} \mathbf{u}^\ell(t) - \mathbf{1}_{I^2\cdot J^2} \mathbf{s}^\ell(t) + (\mathbf{1} - \mathbf{P}^\ell)\mathbf{u}^\ell(t) + (\mathbf{1} - \bar{\mathbf{P}}^\ell)\mathbf{s}^\ell(t) \right) \mathrm{d}t \tag{EC.10}$$

Solving a fluid optimization problem with (EC.11) as the objective is equivalent to maximizing the dynamic index $\mathscr{U}_t^{\text{OW}}$ for all $t \in \mathcal{T}$:

$$\mathscr{U}_t^{\text{OW}} := \sum_\ell \mathbf{P}^\ell \mathbf{u}^\ell(t) + \bar{\mathbf{P}}^\ell \mathbf{s}^\ell(t) \tag{EC.11}$$

EC.2.3. Multi-Objective Framework with More Than Two Objectives

When we have $m \in \mathbb{N}$ $(m > 2)$ objectives in a multi-objective framework, we assign each maximizing objective a non-positive weight and each minimizing objective a non-negative weight. Denote $\boldsymbol{\eta}^1, \ldots, \boldsymbol{\eta}^m$ as the weights for objectives $\text{OBJ}^1, \ldots, \text{OBJ}^m$. Let $\mathbf{w}^1, \ldots, \mathbf{w}^m$ be the weight of penalties for violating (soft) fairness constraints. If we set one of $\mathbf{w}^k, k \in [m]$ to be positive infinity, then we

have a hard fairness constraint. The soft-constraint multi-objective fluid optimization problem is as follows:

$$\min_{(\mathbf{U},\mathbf{S}),\xi\in\mathcal{F}} \quad \mathrm{OBJ}^{\mathrm{Multi}} := \sum_{k=1}^{m} \boldsymbol{\eta}^k \mathrm{OBJ}^k + \left(\sum_{k=1}^{m} \boldsymbol{\eta}^k \mathbf{w}^k\right)^{\top} \int_{t=0}^{T} \boldsymbol{\xi}(t)\,\mathrm{d}t \tag{EC.12}$$

$$s.t. \quad (3)\sim(5),(18),(29) \tag{EC.13}$$

In liver transplantation, reducing (pre-transplant, post-transplant, and total) patient deaths and maximizing QALY are well-accepted objectives. However, these transplantation objectives are not often aligned. When using the multi-objective formulation, it is important to adjust the scale accordingly, which entails estimating the QALY equivalent of saving sick patients from dying. Moreover, this formulation allows us to incorporate input from the transplantation community in choosing the weight parameters.

EC.3. Extensions to the Fluid Models in Section 3

This section discusses extensions to the fluid optimization problems we studied in the main texts. Our fluid model is generic and compatible with various extensions.

EC.3.1. Patient Strategic Behaviors: Multiple Listing

We did not explicitly consider patient strategic behaviors in the base formulation, such as *multiple listing* and endogenous accept/reject decisions in our baseline model. Below, we show that modifying the patient arrival parameters to address multiple listing suffices. Moreover, we can slightly modify our fluid models to incorporate endogenous patient choices as functions of our allocation policy.

Multiple listing (also known as *multi-listing*) refers to the same transplant candidate listing themselves at multiple TCs across different geographical locations, in the hope that they could get a transplant earlier at one of these TCs when a local donor liver becomes available. In our fluid model, we assumed that there is no multi-listing. When allowing multi-listing, there are two cases: In the first case, a patient multi-listed at multiple TCs, but we would categorize them into the same patient group in any one of their listed TC. In this case, it makes no difference whether this patient is multi-listed or not in the fluid model, as this patient belongs to the same patient group. In the second case, a patient may have listed themselves at two TCs and may belong to two patient groups simultaneously. We argue that this case can be fully captured by our fluid model as well, because our fluid model assumes that all patient queues are non-empty, and we do not differentiate patients within the same patient group. Our parameter estimates may change when we factor multi-listing into our model to avoid double counting. That being said, for individual candidates, by multi-listing their chances of getting a transplant earlier increase (as they get more

options); from the central planner's perspective, exactly who in the patient group gets the liver is not a first-order concern and re-estimation of parameters are needed to capture the expected percentages of multi-listing.

EC.3.2. Patient Strategic Behaviors: Endogenous Accept/Reject Decision

EC.3.2.1. Related Work. Transplant candidates' accept/reject decisions on liver offers depend on several factors: their health conditions (e.g. they may need an immediate transplant to sustain life), the suitability of the donor liver (e.g. size and blood/tissue type matching), the cold ischemia time (i.e. time elapsed since harvesting the liver from its deceased donor, the shorter the better), the quality of the liver (e.g. young, healthy donors died from accidents are usually preferred), and the anticipation of future offers (e.g. they may choose to wait for a better offer).

In the literature, researchers have studied patient strategic decisions using discrete, infinite-horizon Markov decision processes (MDPs). For example, Alagoz et al. (2007b) modeled patient accept/decline decision using an MDP and summarized patient decisions based on a) the patient's current and likely future health conditions, b) the current liver offer, and c) the patient's current and future prospects for organ offers. Alagoz et al. (2007) proceeded with structural analysis and Sandıkçı et al. (2008) further found that having a more transparent waiting list helps candidates make better accept/reject decisions. Sandıkçı et al. (2013) formed a partially observable Markov decision process (POMDP) for each candidate, as patient future offer prospects could only be estimated based on aggregated information about the waitlists. In Subsection 6.3, we also briefly discussed related papers using game-theoretic analysis, reduced models, and simulation-based structural models. None of the existing papers solves the analytical, dynamic, and transient optimal organ allocation problem in the presence of patient strategic accept/reject decisions.

While patients' anticipation of future organ offers may be modeled analytically, rigorous empirical studies are needed to investigate whether candidates' accept/reject decisions are truly endogenous and how patients respond to various organ allocation policies.

EC.3.2.2. Discussions on Incorporating Strategic Decisions in Our Fluid Models. Below we show how we can apply the fluid decomposition technique to a case where $\mathbf{P}$ and $\bar{\mathbf{P}}$ are functions of $(\mathbf{U}(t), \mathbf{S}(t))$, i.e., $\mathbf{P}(\mathbf{U}(t), \mathbf{S}(t))$ and $\bar{\mathbf{P}}(\mathbf{U}, \mathbf{S})$. Fluid dynamics equation (6) becomes

$$\dot{\mathbf{x}}(t) = \boldsymbol{\lambda} - \sum_{\ell} \mathbf{P}^{\ell}(\mathbf{U}(t), \mathbf{S}(t))\mathbf{u}^{\ell}(t) - \bar{\mathbf{P}}^{\ell}(\mathbf{U}(t), \mathbf{S}(t))\mathbf{s}^{\ell}(t) + \boldsymbol{\Psi}\mathbf{x}(t) \quad \forall t \tag{EC.14}$$

(14) becomes

$$F(\mathbf{U}(\tau), \mathbf{S}(\tau)) := \lambda - \sum_{\ell} \left(\mathbf{P}^{\ell}(\mathbf{U}(t), \mathbf{S}(t))\mathbf{u}^{\ell}(\tau) + \bar{\mathbf{P}}^{\ell}(\mathbf{U}(t), \mathbf{S}(t))\mathbf{s}^{\ell}(\tau) \right). \tag{EC.15}$$

Note that (13) holds regardless of the explicit form of $F(\mathbf{U}(\tau),\mathbf{S}(\tau))$. Also, (EC.3) $\sim$ (EC.5) all hold under (EC.15) except that $\mathbf{P}$ and $\bar{\mathbf{P}}$ are replaced with the general $\mathbf{P}(\mathbf{U}(t),\mathbf{S}(t))$ and $\bar{\mathbf{P}}(\mathbf{U}(t),\mathbf{S}(t))$. Therefore, we can replace Proposition 3 with the following Proposition EC.2:

PROPOSITION EC.2. *When $\mathbf{\Psi}$ is non-singular and replacing* (6) *with* (EC.15)*, $\mathscr{U}_t^{NPDWT}$ and $\mathscr{U}_t^{QALY}$ can be written as*

$$\mathscr{U}_t^{NPDWT} = \mathbf{d}^\top \left(\exp((T-t)\mathbf{\Psi}) - \mathbf{I}\right) \mathbf{\Psi}^{-1} \left(\sum_\ell \mathbf{P}^\ell(\mathbf{U}(t),\mathbf{S}(t))\mathbf{u}^\ell(t) + \bar{\mathbf{P}}^\ell(\mathbf{U}(t),\mathbf{S}(t))\mathbf{s}^\ell(t) \right) \tag{EC.16}$$

$$\begin{aligned}\mathscr{U}_t^{QALY} = &-\mathbf{q}^\top \left(\exp((T-t)\mathbf{\Psi}) - \mathbf{I}\right) \mathbf{\Psi}^{-1} \left(\sum_\ell \mathbf{P}^\ell(\mathbf{U}(t),\mathbf{S}(t))\mathbf{u}^\ell(t) + \bar{\mathbf{P}}^\ell(\mathbf{U}(t),\mathbf{S}(t))\mathbf{s}^\ell(t) \right) \\ &+ \sum_\ell \mathbf{H}^\ell \mathbf{P}^\ell(\mathbf{U}(t),\mathbf{S}(t))\mathbf{u}^\ell(t) + \bar{\mathbf{H}}^\ell \bar{\mathbf{P}}^\ell(\mathbf{U}(t),\mathbf{S}(t))\mathbf{s}^\ell(t)\end{aligned} \tag{EC.17}$$

Proposition EC.2 shows that the fluid decomposition technique applies to a fluid model with any integrable functions $\mathbf{P}(\mathbf{U}(t),\mathbf{S}(t))$ and $\bar{\mathbf{P}}(\mathbf{U}(t),\mathbf{S}(t))$. This result is powerful, as we are able to remove the differential constraints and reduce the fluid optimization problem over a continuous time horizon to simpler math programs (not necessarily linear programs) to solve optimal decision rules with the presence of endogenous and strategic patient choices. Corollary EC.1 illustrates a case where $\mathbf{P}(\mathbf{U}(t),\mathbf{S}(t))$ and $\bar{\mathbf{P}}(\mathbf{U}(t),\mathbf{S}(t))$ are linear in $(\mathbf{U}(t),\mathbf{S}(t))$.

COROLLARY EC.1. *If $\mathbf{P}^\ell(\mathbf{U}(t),\mathbf{S}(t)) = \mathbf{P}_0 + \mathbf{P}_1 \cdot \mathbf{u}^\ell(t)$ and $\bar{\mathbf{P}}^\ell(\mathbf{U}(t),\mathbf{S}(t)) = \bar{\mathbf{P}}_0 + \bar{\mathbf{P}}_1 \cdot \mathbf{s}^\ell(t)$, $\mathscr{U}_t^{NPDWT}$ and $\mathscr{U}_t^{QALY}$ are quadratic programs, more specifically*

$$\mathscr{U}_t^{NPDWT} = \mathbf{d}^\top \left(\exp((T-t)\mathbf{\Psi}) - \mathbf{I}\right) \mathbf{\Psi}^{-1} \left(\sum_\ell (\mathbf{P}_0 + \mathbf{P}_1 \cdot \mathbf{u}^\ell(t))\mathbf{u}^\ell(t) + (\bar{\mathbf{P}}_0 + \bar{\mathbf{P}}_1 \cdot \mathbf{s}^\ell(t))\mathbf{s}^\ell(t) \right) \tag{EC.18}$$

$$\begin{aligned}\mathscr{U}_t^{QALY} = &-\mathbf{q}^\top \left(\exp((T-t)\mathbf{\Psi}) - \mathbf{I}\right) \mathbf{\Psi}^{-1} \left(\sum_\ell (\mathbf{P}_0 + \mathbf{P}_1 \cdot \mathbf{u}^\ell(t))\mathbf{u}^\ell(t) + (\bar{\mathbf{P}}_0 + \bar{\mathbf{P}}_1 \cdot \mathbf{s}^\ell(t))\mathbf{s}^\ell(t) \right) \\ &+ \sum_\ell \mathbf{H}^\ell (\mathbf{P}_0 + \mathbf{P}_1 \cdot \mathbf{u}^\ell(t))\mathbf{u}^\ell(t) + \bar{\mathbf{H}}^\ell (\bar{\mathbf{P}}_0 + \bar{\mathbf{P}}_1 \cdot \mathbf{s}^\ell(t))\mathbf{s}^\ell(t)\end{aligned} \tag{EC.19}$$

Corollary EC.1 is obtained by directly applying Proposition EC.2.

Notably, our fluid decomposition technique removes (6), placing the term in (6) that is independent of $\mathbf{x}$ and $\dot{\mathbf{x}}$, i.e., $F(\cdot)$, into the decomposed math programs' objective functions. If $F(\cdot)$ is a black-box mapping or a more complex form, solving the decomposed math programs may require advanced optimization methods and techniques well beyond the scope of this paper.

We note that, we do not solve for the exact endogenous form of patients' strategic accept/reject decisions. Our work is complementary to existing work which either formulates the patient MDP

accept/reject decisions (Alagoz et al. 2007) for dynamic decision making or studies the system equilibria (Tunç et al. 2022) for steady-state analysis. In other words, these papers propose the exact forms of $\mathbf{P}(\mathbf{U}(t),\mathbf{S}(t))$ and $\bar{\mathbf{P}}(\mathbf{U}(t),\mathbf{S}(t))$; while our fluid decomposition technique can evaluate policy outcomes for any such forms as long as $F(\cdot)$ is an integrable function.

EC.3.3. Sequential Organ Offering and Provisional Offers

In practice, cadaveric whole livers are offered to waitlisted candidates sequentially. Below we show that sequential liver offering can be easily factored into the fluid model. Suppose a type-ℓ liver is offered to n patients of type ij and each ij-patient's decision is independent of others. With probability π^{ℓ}_{ij}, an ij-patient accept a type-ℓ whole liver offer. Given these notations, we have

$$\mathbf{P}^{\ell}_{ij} = 1-(1-\pi^{\ell}_{ij})^{n} \tag{EC.20}$$

For split livers offered sequentially to n_1 type-ij candidates and n_2 type-$i'j'$ candidates. Each ij-patient's decision is independent of others and with probability $\bar{\pi}^{\ell}_{ij}$, they accept a type-ℓ split liver offer. There are four possible cases:

- Case 1: All patients reject type-ℓ split liver offers. $\Pr(\text{Case 1}) = (1-\bar{\pi}^{\ell}_{ij})^{n_1}(1-\bar{\pi}^{\ell}_{i'j'})^{n_2}$.
- Case 2: At least one type-ij patient accepts a type-ℓ split liver while all type-$i'j'$ patients reject. $\Pr(\text{Case 2}) = \left[1-(1-\bar{\pi}^{\ell}_{ij})^{n_1}\right](1-\bar{\pi}^{\ell}_{i'j'})^{n_2}$.
- Case 3: At least one type-$i'j'$ patient accepts a type-ℓ split liver while all type-ij patients reject. $\Pr(\text{Case 3}) = (1-\bar{\pi}^{\ell}_{ij})^{n_1}\left[1-(1-\bar{\pi}^{\ell}_{i'j'})^{n_2}\right]$.
- Case 4: Both type-ℓ split livers are accepted. $\Pr(\text{Case 4}) = 1-\sum_{i=1}^{3}\Pr(\text{Case } i)$.

We define $\bar{\mathbf{P}}^{\ell}_{ij,i'j'}$ as the probability of at least one partial liver accepts, i.e.,

$$\bar{\mathbf{P}}^{\ell}_{ij,i'j'} = 1-(1-\bar{\pi}^{\ell}_{ij})^{n_1}(1-\bar{\pi}^{\ell}_{i'j'})^{n_2} \tag{EC.21}$$

In Case 1, the liver is usually wasted. In Cases 2 and 3, the liver is likely transplanted to the accepting candidate, using a reduced-size liver transplantation (RLT) technique if necessary.

In some scenarios, a *provisional offer* (i.e. an organ offer before other patients assigned previously declining the same organ), may be extended in order to reduce organ wastage. We can incorporate provisional offers in our fluid model by choosing the corresponding n^P, n^P_1 and n^P_2 that capture the number of total organ offers including provisional offers. No further changes are needed, because eventually, the organ is offered sequentially.

EC.3.4. Broader Geographic Sharing

As UNOS is moving toward a more continuous allocation scoring system (Kasiske et al. 2020, Bertsimas et al. 2020), one important extension to the fluid model is enabling geographic sharing. We can easily incorporate geographic sharing by setting liver and patient categories that include larger

geographical regions within the same group. Note that we cannot guarantee a strictly continuous, boundaryless sharing, as the liver and patient types are categorical by nature in the fluid model; but we can be very close to a continuous one by carefully choosing the parameters that define different liver and patient categories.

EC.3.5. Retransplantation

The retransplantation rate is typically below 10% in liver transplantation (Marudanayagam et al. 2010). Our base model assumes that all patients who accept whole or partial livers leave the waitlist system, regardless of the surgery outcomes: The base model does not explicitly include retransplantation in our model formulation as the retransplantation rate is below 10% (Marudanayagam et al. 2010). Nevertheless, we can easily incorporate retransplantation in our fluid model. The only change is to add $\mathbf{T}^\ell \mathbf{u}^\ell(t) + \bar{\mathbf{T}}\mathbf{s}^\ell(t)$ on the right hand side of (6), where $\mathbf{T}^\ell \in \mathbb{R}^{I \cdot J}$ and $\bar{\mathbf{T}}^\ell \in \mathbb{R}^{I^2 \cdot J^2}$ are the retransplantation probability matrices for WLT and SLT, respectively. In other words, we replace (6) with (EC.22):

$$\dot{\mathbf{x}}(t) = \boldsymbol{\lambda} - \sum_\ell \mathbf{P}^\ell \mathbf{u}^\ell(t) - \bar{\mathbf{P}}^\ell \mathbf{s}^\ell(t) + \boldsymbol{\Psi}\mathbf{x}(t) + \mathbf{T}^\ell \mathbf{u}^\ell(t) + \bar{\mathbf{T}}\mathbf{s}^\ell(t) \quad \forall t \tag{EC.22}$$

EC.3.6. Medical Learning and SLT Expertise

Despite SLT's potential to relieve the acute shortage of donated livers in the US, it is underused in part because few surgeons in the US have learned to perform SLT. One barrier for young surgeons to acquire the skills to perform SLT is the need to perform actual SLT surgeries to become proficient, and the lower success rate such early surgeries have. Further, because SLT is a delicate operation, even with practice, some medical teams may still have only mixed success.

Based on the fluid model and the fluid limit decomposition method described in this work, Tang et al. (2023) study the donated liver allocation problem in a setting where surgeons with different potential abilities may learn SLT, becoming skilled over time. The authors formulate a multi-armed bandit (MAB) model, in which learning curves are embedded in the reward functions, to address the trade-off between discovering and developing talents (exploration) and utilizing a defined group of already-skilled surgeons (exploitation). To solve their MAB learning model, Tang et al. (2023) propose the L-UCB and FL-UCB algorithms, all variants of the upper confidence bound (UCB) algorithm, enhanced with additional features such as learning and fairness. They prove that the regrets of the proposed algorithms, that is, the loss in total rewards due to lack of information about surgeons' aptitudes, are bounded by $O(\log t)$. They also show that the proposed algorithms have superior numerical performance compared to standard bandit algorithms in settings where learning exists. Tang et al. (2023) provide insights into potential strategies to increase the proliferation of SLT and other technically-difficult medical procedures.

EC.4. Sufficient conditions for the interior case

The patient fluid queue lengths in our SLT context are likely always nonempty for several reasons. First, the national liver waitlists are overloaded. Second, the fluid model is a first-order approximation based on FLLN. It is most suitable for strategic planning on a high level with broad patient classes. That entails the proper estimation of model parameters and careful choices of granularity levels.

A sufficient condition for our original fluid optimization problem to stay in the interior of the state space is

$$\lambda_{ij}(t) \geq \sum_{\ell \in \mathcal{L}} \left(P_{ij}^{\ell} \bar{u}_{ij}^{\ell}(t) + \sum_{i',j'} \left(\bar{P}_{ij,(ij,i'j')}^{\ell} \bar{s}_{ij,i'j'}^{\ell}(t) + \bar{P}_{ij,(i'j',ij)}^{\ell} \bar{s}_{i'j',ij}^{\ell}(t) \right) \right) \tag{EC.23}$$

In (EC.23), $\bar{u}_{ij}^{1:L}(t)$, $\bar{s}_{ij,i'j'}^{1:L}(t)$ and $\bar{s}_{i'j',ij}^{1:L}(t)$ are solved for each $i \in \mathcal{I}$ and $j \in \mathcal{J}$ to the following optimization problem for all $t \in \mathcal{T} \setminus \{T\}$, i, and j:

$$\max_{(\mathbf{U}(t),\mathbf{S}(t))} \quad \sum_{\ell \in \mathcal{L}} \left(P_{ij}^{\ell} \bar{u}_{ij}^{\ell}(t) + \sum_{i',j'} \left(\bar{P}_{ij,(ij,i'j')}^{\ell} \bar{s}_{ij,i'j'}^{\ell}(t) + \bar{P}_{ij,(i'j',ij)}^{\ell} \bar{s}_{i'j',ij}^{\ell}(t) \right) \right) \tag{EC.24}$$

$$\bar{\mathbf{u}}^{\ell}(t), \bar{\mathbf{s}}^{\ell}(t) \geq 0 \quad \forall \ell, t \in [0,T] \tag{EC.25}$$

$$\mathbf{1}_{I \cdot J} \bar{\mathbf{u}}^{\ell}(t) + \mathbf{1}_{I^2 \times J^2} \bar{\mathbf{s}}^{\ell}(t) \leq \boldsymbol{\mu}^{\ell}(t) \quad \forall \ell, t \in [0,T] \tag{EC.26}$$

$$\mathbf{1}_{I^2 \cdot J^2} \bar{\mathbf{s}}^{\ell}(t) \leq \bar{\boldsymbol{\mu}}^{\ell}(t) \quad \forall \ell, t \in [0,T] \tag{EC.27}$$

$$\sum_{\ell} \bar{\mathbf{u}}^{\ell}(t) + \sum_{\ell} \mathbf{Z} \bar{\mathbf{s}}^{\ell}(t) \geq \boldsymbol{\Theta} \boldsymbol{\lambda}(t) \quad \forall t \tag{EC.28}$$

The sufficient condition (EC.23) says that the maximum number successful surgeries that can be performed for any wait list cannot meet the incoming demand, subject to capacity and fairness constraints.

EC.5. Application of Our Results to WLT and Kidney Allocation

EC.5.1. Explicit Dynamic Indexes for the Optimal Policy in LT

We first note that if we set $\bar{\boldsymbol{\mu}}^{\ell} = 0$ for all $\ell \in \mathcal{L}$ in (5), then $\mathbf{s}^{\ell} = 0, \forall \ell \in \mathcal{L}$ and therefore the fluid optimization problem (1) $\sim$ (6) reduces to the fluid optimization problem (P_{κ}) in Akan et al. (2012) with $\kappa = 0$. Thus our results yield an exact and explicit solution for solving (P_{κ}) with $\kappa = 0$ in Akan et al. (2012) in the interior case. In a multi-objective framework, i.e., $\kappa \in [0,1]$ in the optimization problem P_{κ} of Akan et al. (2012), solving (P_{κ}) is equivalent to solving the reduced LP (23) $\sim$ (24) with $\bar{\boldsymbol{\mu}}^{\ell} = 0, \forall \ell$.

Akan et al. (2012) derived the dual control problem of (1) $\sim$ (6) and pointed out that the optimal policy could be characterized by the dual solution, i.e., the *shadow prices*. From there, they showed that the optimal policy of the primal problems are dynamic index policies, maximizing indexes that

are functions of the shadow prices. However, the dual control problems which give the indexes are neither smaller or easier than the primal ones, as they contain ordinary differential inequalities in the constraints in addition to linking constraints. Moreover, to obtain the dual solutions, one needs to search through the entire primal dual spaces, for the interior case and the boundary case. Our result show that in the interior of the primal problem's state space, the optimal allocation policy greedily optimizes over decomposed objectives (the dynamic indexes), which compactly summarize the contribution of each action to the overall objective value.

EC.5.2. Structural Properties and Explicit Solutions to Fluid Models in Kidney Allocation

Using our results, the optimal policy of the fluid model that Zenios et al. (2000) used (see their Equation (19)) to describe the kidney allocation system can likewise be decomposed and reduced to standard quadratic programs (QPs). Equity objectives in their work are incorporated into the objective function, instead of appearing in the constraints: This formulation is equivalent to modifying our soft-constraint single-efficiency objective (QALY) with $\mathbf{\Theta} = 0$.

We show that there exists a closed-form expression for their objective (19) and using our fluid-limit decomposition technique, we can find the optimal solution of the proposed fluid model with objective (19) in the interior of the state space. Specifically, we can decompose and reduce the complex fluid control problem to standard QPs, which are solved in polynomial time when the QPs are convex. The optimal policy consists of decision rules that optimize over explicit and finite-dimensional dynamic indexes for each $t \in \mathcal{T}$, and are easy to describe and implement. Moreover, we find analytically tractable optimal decision rules and optimal policies without assumptions or approximations in the interior case.

The quadratic term in Zenios et al. (2000)'s Equation (19) results from their choice of fairness objective. Generally speaking, the choices of fairness concepts (e.g. max-min, envy-free, etc.) should best fit the problem context: The formulation used to mathematically translate these concepts should consider the accuracy in describing the concept, elegance in design/formulation, and computational efficiency.

Below we show the proof. In notation consistent with our previous definitions and compatible with theirs, solving the QP below gives the optimal decision rules at each $t \in \mathcal{T}$:

$$\begin{aligned}\max_{\mathbf{U}(t)} \sum_{\ell} & \gamma^\top \tilde{D}\mathbf{u}^\ell(t) - \beta h^\top \left(\exp((T-t)\mathbf{\Psi}) - \mathbf{I}\right)\mathbf{\Psi}^{-1}\mathbf{P}^\ell\mathbf{u}^\ell(t) \\ & - (1-\beta)\int_t^T \left[\exp((\tau-t)\mathbf{\Psi})(\boldsymbol{\lambda} - \mathbf{P}^\ell\mathbf{u}^\ell(t))\right]^\top \mathbf{R}\left(\exp((\tau-t)\mathbf{\Psi})(\boldsymbol{\lambda} - \mathbf{P}^\ell\mathbf{u}^\ell(t))\right) d\tau \\ & - (1-\beta)\left[\exp[t\mathbf{\Psi}]\mathbf{x}(0)\right]^\top \mathbf{R}\left(\exp((T-t)\mathbf{\Psi}) - \mathbf{I}\right)\mathbf{\Psi}^{-1}(\boldsymbol{\lambda} - \mathbf{P}^\ell\mathbf{u}^\ell) \\ & - (1-\beta)\left[\left(\exp((T-t)\mathbf{\Psi}) - \mathbf{I}\right)\mathbf{\Psi}^{-1}(\boldsymbol{\lambda} - \mathbf{P}^\ell\mathbf{u}^\ell)\right]^\top \mathbf{R}\exp[t\mathbf{\Psi}]\mathbf{x}(0)\end{aligned} \tag{EC.29}$$

$$s.t.\ (3), (4), (6), (18) \tag{EC.30}$$

where $h \in \mathbb{R}^{|\mathcal{I}|\cdot|\mathcal{J}|}$ is defined as the vector of QALY scores assigned to patient groups, $\beta \in [0,1]$ is the weight of the efficiency objective, and $\gamma \in \mathbb{R}^{|\mathcal{I}||\mathcal{J}|}$ is the Lagrange multiplier vector, and $\mathbf{R}$ is an approximated parameter measuring waiting times at the equilibrium allocation rates under the FCFS policy used by Zenios et al. (2000).

Notice that the second line in (EC.29) contains a matrix integral; this can be transformed to closed-form expressions through matrix calculus. Before we dive into the derivation, recall that the matrix $\mathbf{\Psi}$ is based on real data, therefore $\mathbf{\Psi}$ is diagonalizable with probability 1; and it is indeed diagonalizable in our estimation using UNOS/OPTN data from 2009 - 2019. Consistent with our discussion on $\mathbf{\Psi}$'s non-singularity, in the case that $\mathbf{\Psi}$ is not diagonalizable (which occurs with probability 0), we can add a small enough noise matrix/perturbation $\boldsymbol{\epsilon} \in \mathbb{R}^{IJ\times IJ} \to \mathbf{0}$ so that $(\mathbf{\Psi}+\boldsymbol{\epsilon})$ is diagonalizable and $\lim_{\boldsymbol{\epsilon}\to 0} \mathbf{\Psi}+\boldsymbol{\epsilon} = \mathbf{\Psi}$. Summarizing above, we can safely assume that $\mathbf{\Psi}$ is diagonalizable, i.e., there exists a diagonal matrix $\mathbf{D} \in \mathbb{R}^{IJ\times IJ}$ and an invertible matrix $\mathbf{V}$, s.t. $\mathbf{\Psi} = \mathbf{V}^{-1}\mathbf{D}\mathbf{V}$. Note that our proof holds even if Ψ is not diagonalizable; we can use Jordan matrices instead of diagonal $\mathbf{D}$ matrices.

Using the definition of the matrix exponential, we have

$$\begin{aligned} e^{t\mathbf{\Psi}} &= \sum_{k=0}^{\infty} \frac{1}{k!}(t\mathbf{\Psi})^k = \sum_{k=0}^{\infty} \frac{1}{k!}\left(t\boldsymbol{V}^{-1}\boldsymbol{D}\boldsymbol{V}\right)^k = \sum_{k=0}^{\infty} \frac{1}{k!}\boldsymbol{V}^{-1}\left(t\boldsymbol{D}\right)^k\boldsymbol{V} \\ &= \boldsymbol{V}^{-1}\left(\sum_{k=0}^{\infty}\frac{1}{k!}(t\boldsymbol{D})^k\right)\boldsymbol{V} = \boldsymbol{V}^{-1}e^{t\mathbf{D}}\mathbf{V}, \end{aligned}$$

Thus, we know $e^{t\mathbf{\Psi}}$ is also diagonalizable. Therefore, assuming $\beta \in [0,1)$ (the closed-form expression for (EC.29) is trivial when $\beta = 1$), we can equivalently write the second line in (EC.29) as $\sum_\ell \mathbf{A}^\ell$ where $\mathbf{A}^\ell$ is defined as

$$\begin{aligned} &-\frac{1}{1-\beta}\mathbf{A}^\ell \\ &= \int_t^T \left[\exp((\tau-t)\mathbf{\Psi})(\boldsymbol{\lambda}-\mathbf{P}^\ell\mathbf{u}^\ell(t))\right]^\top \mathbf{R}\left(\exp((\tau-t)\mathbf{\Psi})(\boldsymbol{\lambda}-\mathbf{P}^\ell\mathbf{u}^\ell(t))\right)d\tau \\ &= \int_t^T \left[(\mathbf{V}^{-1})\top\exp((\tau-t)\mathbf{D})\mathbf{V}(\boldsymbol{\lambda}-\mathbf{P}^\ell\mathbf{u}^\ell(t))\right]^\top \mathbf{R}\left(\mathbf{V}^{-1}\exp((\tau-t)\mathbf{D})\mathbf{V}(\boldsymbol{\lambda}-\mathbf{P}^\ell\mathbf{u}^\ell(t))\right)d\tau \\ &= (\boldsymbol{\lambda}-\mathbf{P}^\ell\mathbf{u}^\ell(t))^\top\left(\int_t^T \mathbf{V}^\top\exp((\tau-t)\mathbf{D})(\mathbf{V}^{-1})^\top\mathbf{R}\mathbf{V}^{-1}\exp((\tau-t)\mathbf{D})\mathbf{V}d\tau\right)(\boldsymbol{\lambda}-\mathbf{P}^\ell\mathbf{u}^\ell(t)) \end{aligned}$$

Now, we look at the individual elements of $\mathbf{A}^\ell$ and show that we have closed-form expressions for each A_{ij}, $i \in [I], j \in [J]$. For convenience, define $\mathbf{B}^\ell = \int_t^T \mathbf{V}^\top\exp((\tau-t)\mathbf{D})\mathbf{V}^{-1}\mathbf{R}\mathbf{V}^{-1}\exp((\tau-t)\mathbf{D})\mathbf{V}d\tau$. Denote $\mathbf{D}$'s diagonal elements as the scalars d_{kk}, where $k \in \{1,2,\ldots,I\cdot J\}$:

$$B_{ij}^\ell = \sum_{k\in[I],l\in[J]}\int_t^T (\mathbf{V}^\top)_{ik}\exp((\tau-t)d_{kk})\left((\mathbf{V}^{-1})^\top\mathbf{R}\mathbf{V}^{-1}\right)_{kl}\exp((\tau-t)d_{ll})(\mathbf{V})_{lj}d\tau$$

$$= \sum_{k\in[I],l\in[J]} (\mathbf{V}^\top)_{ik} \left((\mathbf{V}^{-1})^\top \mathbf{R}\mathbf{V}^{-1}\right)_{kl} (\mathbf{V})_{lj} \int_t^T \exp((\tau-t)d_{kk}) \exp((\tau-t)d_{ll}) d\tau$$

$$= \sum_{k\in[I],l\in[J]} (\mathbf{V}^\top)_{ik} \left((\mathbf{V}^{-1})\top \mathbf{R}\mathbf{V}^{-1}\right)_{kl} (\mathbf{V})_{lj} \int_t^T \exp((\tau-t)[d_{kk}+d_{ll}]) d\tau$$

$$= \sum_{k\in[I],l\in[J]} (\mathbf{V}^\top)_{ik} \left((\mathbf{V}^{-1})\top \mathbf{R}\mathbf{V}^{-1}\right)_{kl} (\mathbf{V})_{lj} \frac{1}{d_{kk}+d_{ll}} \left[\exp((T-t)(d_{kk}+d_{ll}))-1\right]$$

From the above derivation, we have explicit closed-form expressions for all B_{ij}^ℓ's, where $i \in [I], j \in [J]$. Thus we can write $\mathbf{B}^\ell$ and $\mathbf{A}^\ell$ explicitly. Specifically,

$$\mathbf{A}^\ell = -(1-\beta)(\boldsymbol{\lambda} - \mathbf{P}^\ell \mathbf{u}^\ell(t))^\top \mathbf{B}^\ell (\boldsymbol{\lambda} - \mathbf{P}^\ell \mathbf{u}^\ell(t))$$

And line 2 in (EC.29) can be written in closed-form as follows:

$$\sum_{\ell\in\mathcal{L}} \mathbf{A}^\ell = -\sum_{\ell\in\mathcal{L}} (1-\beta)(\boldsymbol{\lambda} - \mathbf{P}^\ell \mathbf{u}^\ell(t))^\top \mathbf{B}^\ell (\boldsymbol{\lambda} - \mathbf{P}^\ell \mathbf{u}^\ell(t))$$

EC.5.3. Exact Optimal Solution, Reduced Computational Complexity, and Structural Properties

Not only are our solutions exact in the interior space, they also significantly reduce computational complexity. The original fluid control problems have ODEs in the constraints, and such constraints are by nature continuous. Akan et al. (2012) relied on solving the the dual control which requires additional discretization of the dual space for both the interior case and the boundary case.

Besides loss in solution quality as a result of an additional discretization of the continuous dual control problem, one needs to solve a huge discretized LP or QP (Akan et al. 2012, Zenios et al. 2000) with $O(T_N|\mathcal{I}||\mathcal{J}||\mathcal{K}|)$ variables and $O(T_N|\mathcal{I}||\mathcal{J}||\mathcal{K}|)$ constraints for the decision rule at $t \in \mathcal{T}$. While in our decomposed LP, we only need to solve a small LP with $O(|\mathcal{I}||\mathcal{J}||\mathcal{K}|)$ variables and constraints. Note that in practice, $O(|\mathcal{I}||\mathcal{J}||\mathcal{K}|)$ is less than 10^4 even under the most granular classification, but T_N can easily go up to 10^6 scale. Thus, our decomposition results reveal that the fluid model-optimal policy's decision rules are solutions to standard LPs—this finding significantly reduces the complexities of solving the fluid control problem with ODEs in the constraints. Moreover, we can easily derive the optimal decision rule at any $t \in \mathcal{T}$ in the interior of the state space, without the need to discretize the continuous space.

Our decomposed optimal decision rules imply and corroborate the structural properties found in Akan et al. (2012) (i.e. that the optimal policy contains decision rules maximizing some dynamic indexes), and offers a simple and fast approach to find the exact and explicit dynamic indexes without involving the dual control problem. All monotonicity results found in the previous literature become even more clear and straightforward, with our closed-form expressions for the dynamic

indexes (see Section EC.8 in Appendix for detail). We also provide new insights, for example, the convexity and piece-wise linearity of the dynamic index values as functions of resource and fairness constraints. Our exact solutions via fluid limit decomposition illuminate the full potential and inherent properties of the fluid approximation and fluid model-based optimization in organ transplantation.

EC.6. Singular Patient Health Transition Matrix $\mathbf{\Psi}$

When patient health transition matrix $\mathbf{\Psi}$ is estimated from real data numerically, $\mathbf{\Psi}$ is non-singular with very high probability and with probability 1 with infinite precision. Even if we get a singular $\mathbf{\Psi}$, we can add an arbitrarily small perturbation/error matrix to break the singularity, as described in Section 4.

For theoretical completeness, we show that even with a singular $\mathbf{\Psi}$, we can still remove the matrix integration and write the LP objectives (which are functions of $\mathbf{x}(t)$, $\mathbf{u}^\ell(t)$, and $\mathbf{s}^\ell(t)$) in closed form. The only task is to remove the integral of the matrix exponential in the expression for $\mathbf{x}(t)$. When $\mathbf{\Psi}$ is singular, using the Jordan form, we can rewrite it as

$$\mathbf{\Psi} = \mathbf{V}^{-1} \begin{pmatrix} \mathbf{A} & \mathbf{0} \\ \mathbf{0} & \mathbf{B} \end{pmatrix} \mathbf{V}$$

where $\mathbf{B}$ is non-singular, and $\mathbf{A}$ is strictly upper triangular. $\mathbf{V}$ is an invertible matrix. Using the definition of the matrix exponential, we have

$$e^{t\mathbf{\Psi}} = \mathbf{V}^{-1} \begin{pmatrix} e^{t\mathbf{A}} & \mathbf{0} \\ \mathbf{0} & e^{t\mathbf{B}} \end{pmatrix} \mathbf{V}$$

Applying Proposition 3 to the non-singular $\mathbf{B}$, the integral of the matrix exponential above can be written as

$$\int_a^b e^{t\mathbf{\Psi}}\,\mathrm{d}t = \mathbf{V}^{-1} \begin{pmatrix} \int_a^b e^{t\mathbf{A}} dt & \mathbf{0} \\ \mathbf{0} & (e^{b\mathbf{B}} - e^{a\mathbf{B}})\,\mathbf{B}^{-1} \end{pmatrix} \mathbf{V}$$

Denote A's dimension as n (in our problem, $\mathbf{\Psi}$ is a square matrix and its $n = I \cdot J$) Since $\mathbf{A}$ is strictly upper triangular, thus $\mathbf{A}^{n+k} = \mathbf{0}$, $\forall k \in \mathbb{N} \cup \{0\}$. Thus, $\int_0^T e^{t\mathbf{A}} dt$ can be written in closed-form:

$$\begin{aligned} \int_0^T e^{t\mathbf{A}}\,\mathrm{d}t &= T\left(\mathbf{I} + \frac{\mathbf{A}T}{2!} + \frac{(\mathbf{A}T)^2}{3!} + \cdots + \frac{(\mathbf{A}T)^{n-1}}{n!} + \cdots\right) \\ &= T\left(\mathbf{I} + \frac{\mathbf{A}T}{2!} + \frac{(\mathbf{A}T)^2}{3!} + \cdots + \frac{(\mathbf{A}T)^{n-1}}{n!}\right) \end{aligned}$$

Therefore,

$$\int_a^b e^{t\mathbf{A}}\,\mathrm{d}t = \mathbf{I}(b-a) + b\left(\frac{\mathbf{A}b}{2!} + \frac{(\mathbf{A}b)^2}{3!} + \cdots + \frac{(\mathbf{A}b)^{n-1}}{n!}\right) - a\left(\frac{\mathbf{A}a}{2!} + \frac{(\mathbf{A}a)^2}{3!} + \cdots + \frac{(\mathbf{A}a)^{n-1}}{n!}\right)$$

Summarizing above, even when $\mathbf{\Psi}$ is singular, we can still write the objectives of our decomposed LP in closed form.

EC.7. Proofs for Analytical Results in Sections 5 and 6.1

EC.7.1. Proof for Proposition 4

PROPOSITION 4. *The time-varying coefficient vectors in the fluid optimization problems and dynamic indexes are monotonic functions in t: (a) $\mathbf{D}(t)$ and $\bar{\mathbf{D}}(t)$ are nonincreasing in t, and (b) $\mathbf{Q}(t)$ and $\bar{\mathbf{Q}}(t)$ are nondecreasing in t.*

Proof: First, we present two lemmas that will be useful in the proof of monotonicity of the dynamic indices:

LEMMA EC.1. *For a square matrix A and any $t \in \mathbb{R}_{++}$, $\frac{\mathrm{d}e^{tA}}{\mathrm{d}t} = e^{tA}A$.*

LEMMA EC.2. *If matrices A and B commute, i.e., $AB = BA$, then $e^{A+B} = e^A e^B$.*

Let $\mathbf{I}_{IJ,IJ}/\mathbf{I}$ denote the identity matrix of dimension $IJ \times IJ$. Because $\mathbf{I}(\mathbf{\Psi}+\mathbf{I}) = (\mathbf{\Psi}+\mathbf{I})\mathbf{I}$ and $\mathbf{I}^{-1} = \mathbf{I}$; thus $\mathbf{I}^{-1}(\mathbf{\Psi}+\mathbf{I}) = (\mathbf{\Psi}+\mathbf{I})\mathbf{I}^{-1}$, and $(T-t)\mathbf{I}^{-1}(T-t)(\mathbf{\Psi}+\mathbf{I}) = (T-t)(\mathbf{\Psi}+\mathbf{I})(T-t)\mathbf{I}^{-1}$. According to Lemma EC.2, we have $\exp((T-t)\mathbf{\Psi}) = \exp((T-t)(\mathbf{\Psi}+\mathbf{I}-\mathbf{I})) = \exp((T-t)(\mathbf{\Psi}+\mathbf{I}))\exp(-(T-t)\mathbf{I})$.

Given the two lemmas, for $\mathbf{D}(t)$:

$$
\begin{aligned}
\frac{\mathrm{d}\mathbf{D}(t)}{\mathrm{d}t} &= \frac{\mathrm{d}(\mathbf{d}^\top(\exp((T-t)\mathbf{\Psi})-\mathbf{I})\,\mathbf{\Psi}^{-1}\mathbf{P}^\ell)}{\mathrm{d}t} = \frac{\mathrm{d}(\mathbf{d}^\top\exp((T-t)\mathbf{\Psi})\mathbf{\Psi}^{-1}\mathbf{P}^\ell)}{\mathrm{d}t} \\
&= \mathbf{d}^\top\left(\frac{\mathrm{d}(\exp((T-t)\mathbf{\Psi}))}{\mathrm{d}t}\right)\mathbf{\Psi}^{-1}\mathbf{P}^\ell \\
&= \mathbf{d}^\top(-\exp((T-t)\mathbf{\Psi})\mathbf{\Psi})\,\mathbf{\Psi}^{-1}\mathbf{P}^\ell \qquad \text{(apply Lemma EC.1)} \\
&= -\mathbf{d}^\top\exp((T-t)\mathbf{\Psi})\mathbf{P}^\ell \\
&= -\mathbf{d}^\top\exp((T-t)(\mathbf{\Psi}+\mathbf{I}-\mathbf{I}))\mathbf{P}^\ell \\
&= -\mathbf{d}^\top\exp((T-t)(\mathbf{\Psi}+\mathbf{I})-(T-t)\mathbf{I})\mathbf{P}^\ell \\
&= -\mathbf{d}^\top\exp((T-t)(\mathbf{\Psi}+\mathbf{I}))\exp(-(T-t)\mathbf{I})\mathbf{P}^\ell \qquad \text{(Apply Lemma EC.2)}
\end{aligned}
$$

Let us look at $\exp((T-t)(\mathbf{\Psi}+\mathbf{I}))$ in the last line above. Recall that $\mathbf{\Psi}$'s diagonal elements are in $[-1,0)$, while its nondiagonal elements are in $[0,1)$. Thus, all of $(\mathbf{\Psi}+\mathbf{I})$'s elements are in $[0,1)$. As a result, $(\mathbf{\Psi}+\mathbf{I})^k \geq \mathbf{0}$ and $[(T-t)(\mathbf{\Psi}+\mathbf{I})]^k \geq \mathbf{0}$ for any $k \in \mathbb{N}^*$ and $t \in [0,T]$. By definition,

$$\exp((T-t)(\mathbf{\Psi}+\mathbf{I})) = \sum_{k=0}^{\infty}\left[(T-t)(\mathbf{\Psi}+\mathbf{I})\right]^k/k! \geq \mathbf{0}$$

Since $-(T-t)(\mathbf{I})$ is a diagonal matrix, thus $\exp(-(T-t)(\mathbf{I}))$ is also a diagonal matrix and its diagonal elements are $e^{t-T} > 0$. Since $\mathbf{d}$ and $\mathbf{P}^\ell$'s elements are nonnegative, we have

$$\frac{\mathrm{d}\mathbf{D}(t)}{\mathrm{d}t} = -\mathbf{d}^\top\exp((T-t)(\mathbf{\Psi}+\mathbf{I}))\exp(-(T-t)(\mathbf{I}))\mathbf{P}^\ell \leq \mathbf{0}$$

This tells us that $\mathbf{D}(t)$ is nonincreasing in t. Replace $\mathbf{P}^\ell$ with $\bar{\mathbf{P}}^\ell$, the same proof goes through for $\bar{\mathbf{D}}(t)$. Similarly, replace $\mathbf{d}$ above with $(-\mathbf{q})$, we have $\mathbf{Q}(t)$ is nondecreasing. Replacing $\mathbf{d}$ above with $(-\mathbf{q})$ and $\mathbf{P}^\ell$ with $\bar{\mathbf{P}}^\ell$, we get $\bar{\mathbf{Q}}(t)$'s nondecreasing proof.

In proving monotonicity we showed above that $\exp(a\mathbf{\Psi}) > 0$ for any $a \geq 0$. This also implies that the NPDWT dynamic index is nonnegative:

$$\mathscr{U}_t^{\text{NPDWT}} := \mathbf{d}^\top \left\{ \int_t^T \exp[(\tau - t)\mathbf{\Psi}]\, \mathrm{d}\tau \right\} \left(\sum_\ell \mathbf{P}^\ell \mathbf{u}^\ell(t) + \bar{\mathbf{P}}^\ell \mathbf{s}^\ell(t) \right) \geq \mathbf{0}$$

The first term in the QALY dynamic index is nonpositive:

$$-\sum_\ell \mathbf{q}^\top \left\{ \int_t^T \exp[(\tau - t)\mathbf{\Psi}]\, \mathrm{d}\tau \right\} \left(\mathbf{P}^\ell \mathbf{u}^\ell(t) + \bar{\mathbf{P}}^\ell \mathbf{s}^\ell(t) \right) \leq \mathbf{0}$$

Proposition 4 essentially tells us that as t increases, the absolute values of dynamic indices's coefficient vectors shrink. This suggests earlier allocation decisions have a larger impacts in absolute value on the cumulative system objective value.

EC.7.2. Proof for Proposition 5

PROPOSITION 5. *The any-t instantaneous fairness constraint* (28) *is equally or more strict compared to the cumulative fairness constraint* (38)*, under the same fairness level $\mathbf{\Theta}$, and assuming the patient arrival rates is time-independent (i.e., $\boldsymbol{\lambda}(t) \equiv \boldsymbol{\lambda}$).*

Proof: Let $\mathbf{U}, \mathbf{S}$ satisfy the any-t fairness constraint (28) with fairness level $\mathbf{\Theta}$. That is,

$$\sum_\ell \mathbf{u}^\ell(t) + \sum_\ell \mathbf{Z}\mathbf{s}^\ell(t) \geq \mathbf{\Theta}\boldsymbol{\lambda} \quad \forall t$$

Plugging this to the LHS of inequality (38) gives

$$\int_{t=0}^T \left(\sum_\ell \mathbf{u}^\ell(t) + \sum_\ell \mathbf{Z}\mathbf{v}^\ell(t) \right) \mathrm{d}t \geq \int_{t=0}^T \mathbf{\Theta}\boldsymbol{\lambda}\, \mathrm{d}t = \mathbf{\Theta}\boldsymbol{\lambda} T$$

which gives us the cumulative fairness constraint (38). Q.E.D.

EC.7.3. Proof for Proposition 6

PROPOSITION 6. *$f(\boldsymbol{\mu}^1, \ldots, \boldsymbol{\mu}^{|\mathcal{L}|}, \bar{\boldsymbol{\mu}}^1, \ldots, \bar{\boldsymbol{\mu}}^{|\mathcal{L}|}, \mathbf{\Theta}\boldsymbol{\lambda}, \boldsymbol{\lambda})$ is jointly concave.*

Proof: Recall that $\boldsymbol{\mu}^\ell(t) \in \mathbb{R}_+^{I \cdot J}, \bar{\boldsymbol{\mu}}^\ell(t) \in [\mathbf{0}, \boldsymbol{\mu}^\ell(t)], \mathbf{\Theta} \in [0,1]^{I \cdot J}, \boldsymbol{\lambda}(t) \in \mathbb{R}_+^{I \cdot J}, \forall \ell \in \mathcal{L}, t \in \mathcal{T}$. The feasible set of $f(\cdot)$ is convex. We first prove that $g_t^{\text{Multi}}(\boldsymbol{\mu}^\ell, \bar{\boldsymbol{\mu}}^\ell, \mathbf{\Theta}\boldsymbol{\lambda}, \boldsymbol{\lambda}, \ell \in \mathcal{L}) := \max_{(\mathbf{U},\mathbf{S})} \mathscr{U}_t^{\text{Multi}}$ is piece-wise linear concave in the RHS (e.g. $\boldsymbol{\mu}^\ell, \bar{\boldsymbol{\mu}}^\ell, \mathbf{\Theta}\boldsymbol{\lambda}, \boldsymbol{\lambda}, \ell \in \mathcal{L}$). The proof follows the global sensitivity analysis from Bertsimas and Tsitsiklis (1997) (see their Section 5.2, Equation 5.2). According to our fluid limit decomposition in the fully overloaded setting and the exchangeability in integration dimensions (EC.5), $\text{OBJ}^{\text{Multi}}$ is a definite integral of $g_t^{\text{Multi}}(\boldsymbol{\mu}^\ell, \bar{\boldsymbol{\mu}}^\ell, \mathbf{\Theta}\boldsymbol{\lambda}, \boldsymbol{\lambda}, \ell \in \mathcal{L})$ from 0 to T. Concavity is preserved by integrals (Boyd et al. 2004). Q.E.D.

EC.7.4. Proof for Corollary 1

COROLLARY 1. *The marginal benefit of an additional liver is monotonically non-increasing in* $\boldsymbol{\mu}$ *and* $\bar{\boldsymbol{\mu}}$.

Proof: According to Proposition 6, $f(\boldsymbol{\mu}^1 \ldots, \boldsymbol{\mu}^{|\mathcal{L}|}, \bar{\boldsymbol{\mu}}^1, \ldots, \bar{\boldsymbol{\mu}}^{|\mathcal{L}|}, \boldsymbol{\Theta\lambda}, \boldsymbol{\lambda})$ is concave, thus $\frac{\partial f(\boldsymbol{\mu}^1,\ldots,\boldsymbol{\mu}^{|\mathcal{L}|},\bar{\boldsymbol{\mu}}^1,\ldots,\bar{\boldsymbol{\mu}}^{|\mathcal{L}|},\boldsymbol{\Theta\lambda},\boldsymbol{\lambda})}{\partial \boldsymbol{\mu}}$ (the marginal benefit of one additional donor liver) is monotonically non-increasing in $\boldsymbol{\mu}$, and $\frac{\partial f(\boldsymbol{\mu}^1,\ldots,\boldsymbol{\mu}^{|\mathcal{L}|},\bar{\boldsymbol{\mu}}^1,\ldots,\bar{\boldsymbol{\mu}}^{|\mathcal{L}|},\boldsymbol{\Theta\lambda},\boldsymbol{\lambda})}{\partial \bar{\boldsymbol{\mu}}}$ (the marginal benefit of one additional split-table donor liver) is monotonically non-increasing in $\bar{\boldsymbol{\mu}}$.

EC.7.5. Proof for Corollary 2

COROLLARY 2. *With* $\boldsymbol{\lambda}$ *fixed,* PoF($\boldsymbol{\Theta}$) *is monotonically non-decreasing and convex in* $\boldsymbol{\Theta}$*, over* (32) $\sim$ (33)*'s feasible range.*

Proof: First, because the larger $\boldsymbol{\Theta} \geq 0$ is, the more restrictive (29) is, the smaller the feasible set the LP (23) $\sim$ (24) has. As a result, the objective function value (23) potentially decreases, thus $f(\boldsymbol{\mu}^1, \ldots, \boldsymbol{\mu}^{|\mathcal{L}|}, \bar{\boldsymbol{\mu}}^1, \ldots, \bar{\boldsymbol{\mu}}^{|\mathcal{L}|}, \boldsymbol{\Theta\lambda}, \boldsymbol{\lambda})$ potentially goes down when $\boldsymbol{\Theta}$ increases. Therefore, PoF $= 1 - \frac{f(\boldsymbol{\mu}^1,\ldots,\boldsymbol{\mu}^{|\mathcal{L}|},\bar{\boldsymbol{\mu}}^1,\ldots,\bar{\boldsymbol{\mu}}^{|\mathcal{L}|},\boldsymbol{\Theta\lambda},\boldsymbol{\lambda})}{f(\boldsymbol{\mu}^1,\ldots,\boldsymbol{\mu}^{|\mathcal{L}|},\bar{\boldsymbol{\mu}}^1,\ldots,\bar{\boldsymbol{\mu}}^{|\mathcal{L}|},\mathbf{0},\boldsymbol{\lambda})}$ is non-decreasing.

According to Proposition 6, $f(\boldsymbol{\mu}^\ell, \bar{\boldsymbol{\mu}}^\ell, \boldsymbol{\Theta}, \boldsymbol{\lambda})$ is concave. Because $f(\boldsymbol{\mu}^\ell, \bar{\boldsymbol{\mu}}^\ell, \mathbf{0}, \boldsymbol{\lambda}) > 0$ is a fixed number, $\frac{f(\boldsymbol{\mu}^1,\ldots,\boldsymbol{\mu}^{|\mathcal{L}|},\bar{\boldsymbol{\mu}}^1,\ldots,\bar{\boldsymbol{\mu}}^{|\mathcal{L}|},\boldsymbol{\Theta\lambda},\boldsymbol{\lambda})}{f(\boldsymbol{\mu}^1,\ldots,\boldsymbol{\mu}^{|\mathcal{L}|},\bar{\boldsymbol{\mu}}^1,\ldots,\bar{\boldsymbol{\mu}}^{|\mathcal{L}|},\mathbf{0},\boldsymbol{\lambda})}$ is concave, and PoF $= 1 - \frac{f(\boldsymbol{\mu}^1,\ldots,\boldsymbol{\mu}^{|\mathcal{L}|},\bar{\boldsymbol{\mu}}^1,\ldots,\bar{\boldsymbol{\mu}}^{|\mathcal{L}|},\boldsymbol{\Theta\lambda},\boldsymbol{\lambda})}{f(\boldsymbol{\mu}^1,\ldots,\boldsymbol{\mu}^{|\mathcal{L}|},\bar{\boldsymbol{\mu}}^1,\ldots,\bar{\boldsymbol{\mu}}^{|\mathcal{L}|},\mathbf{0},\boldsymbol{\lambda})}$ is convex.

EC.7.6. Proof for Proposition 7

PROPOSITION 7. *For each splittable liver type* $\ell \in \mathcal{L}$*, only split an incoming liver of this type if* $\exists\, i, i' \in \mathcal{I}, j, j' \in \mathcal{J}$*, s.t. (a)* $\bar{D}^\ell_{ij,i'j'}(t) \geq \max_{i'',j''} D^\ell_{i''j''}(t)$*, and b)* $\bar{Q}^\ell_{ij,i'j'}(t) \geq \max_{i'',j''} Q^\ell_{i''j''}(t)$*, the optimal policy (w.r.t* (32)*, for any* κ*) tends to split as the incoming* ℓ *liver at* t *(subject to* (5)*,* (28)*, and* (18)*).*

Proof: Based on the explicit objective function of LP (23) $\sim$ (24), when $\bar{\mathbf{D}}^\ell_{ij,i'j'}(t) \geq \max_{i'',j''} \mathbf{D}^\ell_{i''j''}(t)$ and $\bar{\mathbf{Q}}^\ell_{ij,i'j'}(t) \geq \max_{i'',j''} \mathbf{Q}^\ell_{i''j''}(t)$ hold, the coefficient of splitting ℓ and transplanting it to $(ij, i'j')$ dominates, thus the objective value of a decision rule that allocates as many type-ℓ livers as possible to a $(ij, i'j')$-pair for SLT is higher than that of a decision rule allocates more-than-necessary type-ℓ livers for WLT. Constraint (5) ensures that the allocation does not exceed the splittable-liver capacity; this constraint is ordinary and thus won't affect the optimal splitting decisions. (28) prevents the allocation from infringing the fairness guarantee; under certain choices of $\boldsymbol{\Theta}$, this could mean forcing the decision rules to deviate from the optimal splitting decisions without fairness constraints. (18) assures that the fluid limits to always stay non-negative (i.e. never assign livers to empty fluid queues). This constraint is not active in the interior case; for completeness, we include it here and it serves as a constraint for the boundary case heuristics.

EC.7.7. Proof for Corollary 3

COROLLARY 3. *If for every liver type $\ell \in \mathcal{L}$ that is medically safe to be used for SLT, $\exists\, i, i' \in \mathcal{I}, j, j' \in \mathcal{J}$, s.t. (a) $\bar{D}^{\ell}_{ij,i'j'}(t) \geq \max_{i'',j''} D^{\ell}_{i''j''}(t)$, and b) $\bar{Q}^{\ell}_{ij,i'j'}(t) \geq \max_{i'',j''} Q^{\ell}_{i''j''}(t)$, the optimal policy (w.r.t* (32)*, for any κ) splits all splittable liver at t (subject to* (5), (28)*, and* (18)*).*

Proof: When for all $\ell \in \mathcal{L}$, $\exists\, i, i' \in \mathcal{I}, j, j' \in \mathcal{J}$, s.t. (a) $\bar{\mathbf{D}}^{\ell}_{ij,i'j'}(t) \geq \max_{i'',j''} \mathbf{D}^{\ell}_{i''j''}(t)$, and b) $\bar{\mathbf{Q}}^{\ell}_{ij,i'j'}(t) \geq \max_{i'',j''} \mathbf{Q}^{\ell}_{i''j''}(t)$ hold, apply Proposition 7: The coefficient of splitting ℓ and transplanting it to their corresponding $(ij, i'j')$ dominates. Thus, for every ℓ, the objective value of a decision rule that allocates as many type-ℓ livers as possible to their corresponding $(ij, i'j')$-pair for SLT is higher than that of a decision rule allocates more-than-necessary type-ℓ livers for WLT. Of course, the decision rules are subject to the other constraints and may have to deviate from always splitting at some t's. Please refer to the proof for Proposition 7 for discussions on the influences of constraints.

EC.8. Analytical Results Analogous to Propositions 1 and 2 from Akan et al. (2012)

With our closed-form objective functions and constraints, we can solve the decomposed LPs with standard solvers and perform sensitivity analysis on the optimal decision rules using the explicit LPs. For example, if we want to study the impact of increasing d^{ℓ}_{ij} or H^{ℓ}_{ij} on our optimal decision: when we increase/decrease the parameters just a little bit, the base of the solution may not change; however, our optimal solution and the base may change when we further increase/decrease the parameters to some point. Below we present two corollaries analogous to Propositions 1 and 2 from-Akan et al. (2012) but in our fluid formulation with SLT and fairness. Note that we only demonstrate a subset of sufficient conditions, more general results are possible.

The UNOS policies usually give precedence to the sickest patients. Corollary EC.2 characterizes sufficient scenarios where such a strategy is optimal in minimizing patient deaths on the waitlists. Corollary EC.2 is not a direct translation or extention of Proposition 1 from Akan et al. (2012) in our context, due to the difference in formulation of the transition matrix $\mathbf{\Psi}$, but it provides comparable and broader insights.

COROLLARY EC.2. *Suppose that $P^{\ell}_{ij} = P^{\ell}_{i'j} = P^{\ell}_{j}$ for all i, i', j, ℓ for WLT, $\bar{\mathbf{P}}^{\ell}_{:,(ij,i'j')} = \bar{\mathbf{P}}^{\ell}_{:,(i''j,i'''j')} = \bar{\mathbf{P}}^{\ell}_{(j,j')}$, and $\bar{\mathbf{P}}^{\ell}_{:,(i'j',ij)} = \bar{\mathbf{P}}^{\ell}_{:,(i'''j',i''j)} = \bar{\mathbf{P}}^{\ell}_{(j',j)}$ for SLT, $\forall i, i', i'', i''', j, j', \ell$. In an optimal solution to* (1) $\sim$ (6)*, within the same static group, patients' relative priorities are set in the order of their death rates $\mathbf{d}$, i.e., giving the priority to the sickest patients (who are mostly likely to die in the next 90 days), provided that $d_{ij} > d_{i(j-1)}, \forall i, j = \{2, \ldots, J\}$ and $\mathbf{y} := \mathbf{d}^{\top} \left(\exp((T-t)\mathbf{\Psi}) - \mathbf{I}\right) \mathbf{\Psi}^{-1} \in \mathbb{R}^{1 \times IJ}$ satisfies $y_{ij} > y_{i(j-1)}, \forall i, j = \{2, \ldots, J\}$, $\forall t \in (0, T-t]$.*

The proof of Corollary EC.2 uses the decomposed dynamic indexes. The high-level idea is that $\mathbf{y}$ summarizes the total reduced deaths (including the immediate removals and the reduced future deaths as a result of shortened waitlists) from t to T per unit of liver allocated to each of the patient classes.

Proof: Because $d_{ij} > d_{i(j-1)}, \forall i, j = \{2, \ldots, J\}$ and $y_{ij} > y_{i(j-1)}, \forall i, j = \{2, \ldots, J\}$, $\forall t \in (0, T-t]$ and the assumptions on $\mathbf{P}$ and $\bar{\mathbf{P}}$, $\mathbf{C} := \mathbf{d}^\top \left(\exp((T-t)\boldsymbol{\Psi}) - \mathbf{I}\right) \boldsymbol{\Psi}^{-1} \mathbf{P} \in \mathbb{R}^{1 \times IJ}$ and $\bar{\mathbf{C}} := \mathbf{d}^\top \left(\exp((T-t)\boldsymbol{\Psi}) - \mathbf{I}\right) \boldsymbol{\Psi}^{-1} \bar{\mathbf{P}} \in \mathbb{R}^{1 \times IJ}$ satisfy: $C_{ij} > C_{i(j-1)}$, $\bar{C}_{ij,i'j'} > C_{i(j-1),i'j'}$, and $\bar{C}_{i'j',ij} > C_{i'j',i(j-1)}$, $\forall i, i', j, j', t$ and $j \in \{2, \ldots, J\}$. Therefore, the marginal benefit or the weight of class ij is larger than that of patient class $i(j-1)$, for all $i, j \in \{2, \ldots, J\}$; the optimal solution will prioritize those patient classes with larger marginal benefit, equivalently, the sickest under the premises of Corollary EC.2 Q.E.D..

The UNOS policies sometimes prioritize certain static patient groups when other conditions are the same, e.g. children over adults. Corollary EC.3 characterize when such policies are optimal and generalizes Proposition 2 from Akan et al. (2012).

COROLLARY EC.3. *Suppose that there exists a permutation $r^\ell(\cdot)$ of $\mathcal{I}$ such that $q^\ell_{r^\ell(1)j} \geq q^\ell_{r^\ell(2)j} \geq \cdots \geq q^\ell_{r^\ell(I)j}$ for all $j \in \mathcal{J}, \ell \in \mathcal{L}$, and for each $\ell \in \mathcal{L}$, and a subset of the following conditions holds*

$$H^\ell_{r^\ell(1)j} \geq H^\ell_{r^\ell(2)j} \geq \cdots \geq H^\ell_{r^\ell(I)j}, \quad \forall j \in \mathcal{J} \tag{EC.31}$$

$$\bar{H}^\ell_{r^\ell(1)j,i'j'} \geq \bar{H}^\ell_{r^\ell(2)j,i'j'} \geq \cdots \geq \bar{H}^\ell_{r^\ell(I)j,i'j'}, \quad \forall j, j' \in \mathcal{J}, i' \in \mathcal{I} \tag{EC.32}$$

$$\bar{H}^\ell_{i'j',r^\ell(1)j} \geq \bar{H}^\ell_{i'j',r^\ell(2)j} \geq \cdots \geq \bar{H}^\ell_{i'j',r^\ell(I)j}, \quad \forall j, j' \in \mathcal{J}, i' \in \mathcal{I} \tag{EC.33}$$

$$P^\ell_{r^\ell(1)j} \geq P^\ell_{r^\ell(2)j} \geq \cdots \geq P^\ell_{r^\ell(I)j}, \quad \forall j \in \mathcal{J} \tag{EC.34}$$

$$\bar{\mathbf{P}}^\ell_{:,(r^\ell(1)j,i'j')} \geq \bar{\mathbf{P}}^\ell_{:,(r^\ell(2)j,i'j')} \geq \cdots \geq \bar{\mathbf{P}}^\ell_{:,(r^\ell(I)j,i'j')}, \quad \forall j, j' \in \mathcal{J}, i' \in \mathcal{I} \tag{EC.35}$$

$$\bar{\mathbf{P}}^\ell_{:,(i'j',r^\ell(1)j)} \geq \bar{\mathbf{P}}^\ell_{:,(i'j',r^\ell(2)j)} \geq \cdots \geq \bar{\mathbf{P}}^\ell_{:,(i'j',r^\ell(I)j)}, \quad \forall j, j' \in \mathcal{J}, i' \in \mathcal{I} \tag{EC.36}$$

a. If (EC.31) *and* (EC.34) *hold, $H^\ell_{r^\ell(1)j} > \bar{H}^\ell_{r^\ell(1)j,i'j'} + \bar{H}^\ell_{i'j',r^\ell(1)j}$, and for any i, i', j, j', $P^\ell_{r^\ell(1)j} > \max\{\bar{P}^\ell_{r^\ell(1)j,i'j'}, \bar{P}^\ell_{i'j',r^\ell(1)j}\}$, an optimal solution to* (7) $\sim$ (8) *only assigns livers of type ℓ to static patient type $r^\ell(1) = \arg\max_i H^\ell_{ij}$ if $x_{ij} > 0$ for all i, j and $t \in \mathcal{T}$.*

b. If (EC.32) *and* (EC.35) *hold, and for any i, i', j, j', $\bar{H}^\ell_{r^\ell(1)j,i'j'} > H^\ell_{r^\ell(1)j}$, and $\bar{P}^\ell_{r^\ell(1)j,i'j'} > P^\ell_{r^\ell(1)j}$, an optimal solution to* (7) $\sim$ (8) *only assigns partial livers of type ℓ to static patient type $r^\ell(1) = \arg\max_i \bar{H}^\ell_{ij}$ as primary recipients if $x_{ij} > 0$ $\forall i, j$ and $t \in \mathcal{T}$.*

c. If (EC.33) *and* (EC.36) *hold, and for any i, i', j, j', $\bar{H}^\ell_{i'j',r^\ell(1)j} > H^\ell_{r^\ell(1)j}$, and $\bar{P}^\ell_{i'j',r^\ell(1)j} > P^\ell_{r^\ell(1)j}$, an optimal solution to* (7) $\sim$ (8) *only assigns partial livers of type ℓ to static patient type $r^\ell(1) = \arg\max_i \bar{H}^\ell_{ij}$ as secondary recipients if $x_{ij} > 0$ $\forall i, j$ and $t \in \mathcal{T}$.*

The proof is straight-forward, because between static classes there is no transition. Therefore, we can ignore $\boldsymbol{\Psi}$ in (19) $\sim$ (20) and based on the explicit LP formulation, draw the monotonicity conclusions directly.

EC.9. Current SLT practice

For completeness, we describe the practice of SLT in the US and more specifically, at the world-renowned transplant center where two of the authors work.

EC.9.1. Two Splitting Methods for SLT

There are two splitting methods and a liver can only be split once, according to the OPTN white paper (OPTN and UNOS 2016):

- An adult-child split. In this splitting method, a small child or very small-statured adult receives the smaller left lobe, and an adult receives the extended right lobe.
- An adult-adult (or adult-big child) split where an adult receives the right lobe, and an adult (or big child) receives the left lobe.

Current SLT practice indicates that the adult-child split is consistently favorable. Nevertheless, recent reports indicated good results could be achieved in relatively healthier recipients and advanced techniques (OPTN and UNOS 2016).

EC.9.2. SLT Expertise

In the US, after graduating from medical schools and having chosen their specialization areas, surgeons complete their residency programs to obtain an unrestricted license to practice medicine and a board certificate for their chosen surgical specialty, in our case, the liver transplant. It is during residency that surgeons may learn SLTs at selected TCs, such as the one at University of California, San Francisco.

EC.9.3. The Liver Allocation Procedure and SLT Use as Exceptional Cases

In practice, successful SLTs involve a complicated process, including registration, procurement, allocation, logistics, surgical operations, and post-surgery recovery. To start, eligible ESLD patients choose transplant centers and register for the national liver transplant waitlists. When a deceased-donor liver becomes available and is being evaluated to determine whether it is medically splittable (based on donor age, body mass index, size, etc.), UNOS generates a ranked list (known as the *match-run*), based on computerized algorithms. The organ is offered to the match-run candidates sequentially, until a candidate/candidate pair accepts it. The longer it takes between the removal of blood supply from the deceased-donor organ and the transplantation into the recipient(s) (the *cold ischemia time*), the more the organ's quality deteriorates. An organ is discarded if the cold ischemia time is determined to be too long (exceeding 12 - 18 hours).

Once a liver is accepted, the organ is harvested (and split if to be used in SLTs) by a trained team at the donor hospital. The matching of transplant surgeons and candidates is finalized after a candidate has accepted an offer and right before the surgery. After being harvested, the procured whole liver (two split liver grafts) is transported to the WLT patient TC (SLT patient TCs), where

the WLT surgery (SLT surgeries) is performed by the patient's transplant surgeon, and patient recovery occurs.

Currently, most SLTs are performed in few major transplant centers; thus, the primary recipients (usually children) and secondary recipients are usually within the same TC (Ge et al. 2020). However, because of UNOS's new acuity circles policy that took effect in 2019 (UNOS system notice: Liver and intestinal organ distribution based on acuity circles implemented February 4, 2020, https://unos.org/news/system-implementation-notice-liver-and-intestinal-organ-distribution-based-on-acuity-circles-implemented-feb-4/), patients from different TCs within the acuity circles may receive halves of the same donor liver more frequently. Researchers are also exploring continuous distribution that do not rely on geographical boundaries (Bertsimas et al. 2020, Kasiske et al. 2020).

EC.10. More on Numerical Experiments

EC.10.1. More on the Experiment Setup

In the first set of experiments, we compare the objective values of the optimal solution (the "fluid optimal") with objective values of (32) under alternative policies. This experiment focuses on the structural properties of the "fluid optimal" policy and captures only the first-order dynamics of the liver wait lists.

In our second experiment, we set up a discrete simulation model for a 1-year time horizon. Liver and patient arrivals in each discrete time step follow Poisson Distribution; and patient deaths, transitions, and removals follow a Binomial distribution. All parameters are calibrated to available data. Please note that $\boldsymbol{\Theta} = \mathbf{0}$ in this set of experiments, as we evaluate and compare alternative policies in a simulated environment reflecting current practice, where no fairness measures regarding sizes are in place. Each simulation run is a sample path, and we generate Figure 6 using five runs for each box. The simulation model mimics the liver allocation system and incorporates higher-order dynamics.

EC.10.2. Additional Numerical Experiment Results

EC.10.3. Additional Discussions on Our Numerical Experiments

The improvement of our "optimal split, optimal allocation" policy over other policies that do not utilize SLT likely gives a conservative estimate of the potential of SLTs to achieve multiple liver transplantation goals, because in reality $> 10\%$ of donated livers are splittable (OPTN and UNOS 2016), yet we assume $\bar{\boldsymbol{\mu}} = 0.1\boldsymbol{\mu}$ as there is no consensus on the exact percentage of splittable livers.

As already mentioned, "all-split, optimal allocation" performs nearly as well at maximizing QALY and MULTI, and minimizing NPDWT; this similarity in performance is driven by the fact that the "optimal split, optimal allocation" strategy splits more than 99% of medically-splittable livers in the simulation.

EC.10.4. Additional Numerical Experiments Testing the Robustness to System Parameters

We next study the effect of the imbalance among patient and liver size groups in terms of arrival rates. To simulate imbalance in size, we modify the patient arrival rates and liver arrival rates adversarially. Specifically, we let f be an adjustment factor, taking value from $\{-20\%, -10\%, 0\%, 10\%, 20\%\}$. We then multiply the arrival rates of S, M, ML, and L livers by $100\% + f$, $100\% + f/3$, $100\% - f/3$, and $100\% - f$, respectively. Similarly, We then multiply the arrival rates of S, M, ML, and L patients by $100\% - f$, $100\% - f/3$, $100\% + f/3$, and $100\% + f$, respectively. For example, with $f = -20\%$, we decrease the arrival rates of S livers and L patients by 20% and increase the arrival rates of L livers and S patients by 20%. As shown in Figure EC.3, a larger f negatively impacts both objectives, whereas SLTs still exhibit robust and clear benefits in all experiments.

We also examine the number of livers allocated to each patient size group. Such analyses help interpret the optimal solutions and illustrate how system parameters affect (split) liver allocation decisions. Figure EC.4 shows the numbers of whole and split livers allocated to all four patient size groups under five scenarios in which we apply multiplicative factors to the patient arrival rates, following the same settings as in Figure EC.3. The transplantation objective is to maximize QALY. Results reveal that the "optimal split, optimal allocation" policy allocates roughly the same numbers of whole and split livers to all size groups, indicating that "all-split, optimal allocation" remains near-optimal despite parameter changes. In terms of allocation decisions across patient size groups, "optimal split, optimal allocation" and "all-split, optimal allocation" assign the greatest

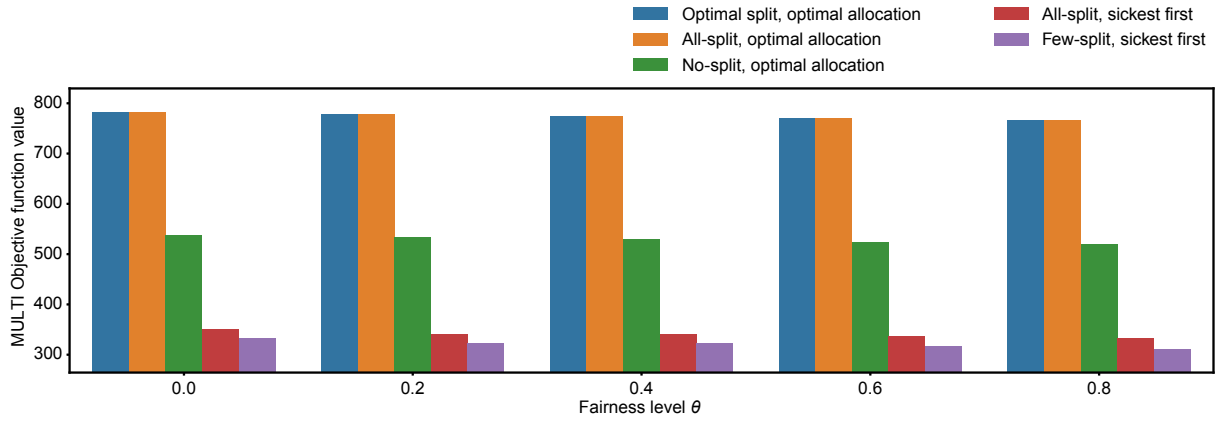

Figure EC.1 **Comparisons of five policies under the maximizing multi-objective where $\kappa = 0.01$. We compare the same five policies discussed in Section 7: The "all-split, optimal allocation" policy seems to perform as well as "optimal-split, optimal allocation" and dominates other policies. "All-split, sickest first" consistently outperforms "few-split, sickest first." The benefits of wider use of SLT appear to be more significant in "optimal allocation" policies.**

numbers of livers (whole or partial) to small patients compared with the other policies. "No-split, optimal allocation" assigns more livers to the S patient group compared to the "sickest first" policies. When the multiplicative factor grows larger, which indicates access to liver transplants for smaller patients increases, more livers are then given to physically larger patients as splitting becomes less necessary. Under the two "sickest-first" policies, the numbers of livers allocated to small patients are the lowest among all policies, whereas the L patient group consistently receives more livers.

We now study the effect of queue length by modifying the initial queue lengths using two approaches. In the first approach (Figure EC.5), we multiply the initial lengths of all queues by a factor of 50%, 100%, and 200%. In the second approach (Figure EC.6), we modify the initial lengths of queues differently: we modify the initial queue lengths of small, healthy patients and

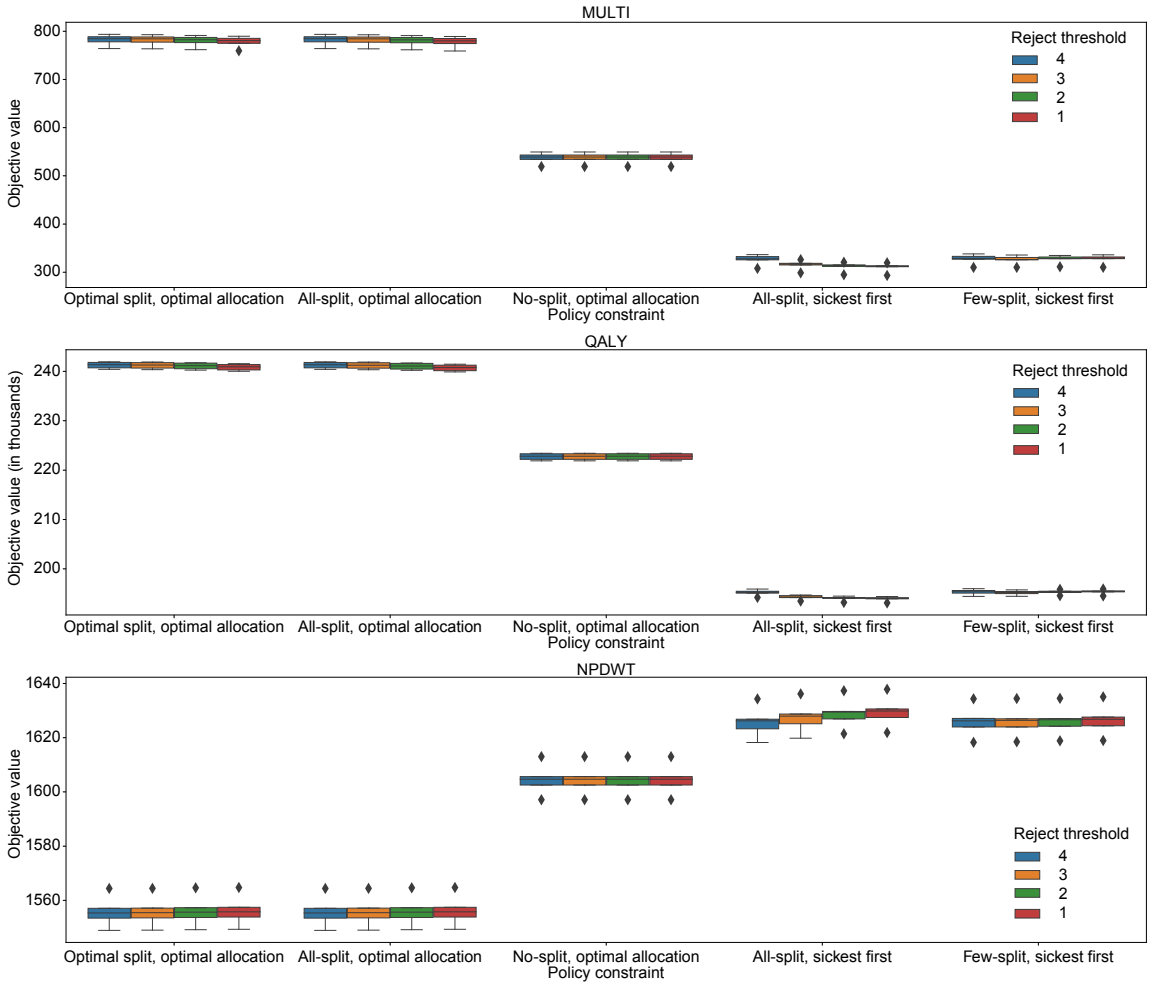

Figure EC.2 **Simulation results based on OPTN data: We experiment with smaller reject thresholds in this experiment. Smaller reject thresholds indicate worse objective values. The "all-split, sickest first" policy seems the most sensitive to strategic behaviors.**

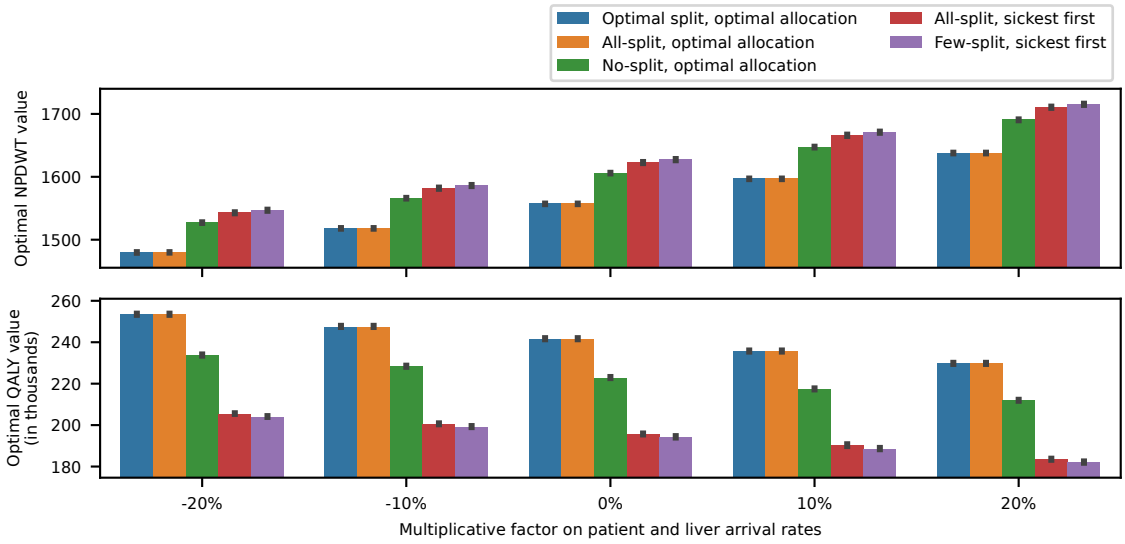

Figure EC.3 **Comparison of five policies in five simulated settings with different patient and liver arrival rates, simulating various degrees of imbalance between patient and liver sizes.**

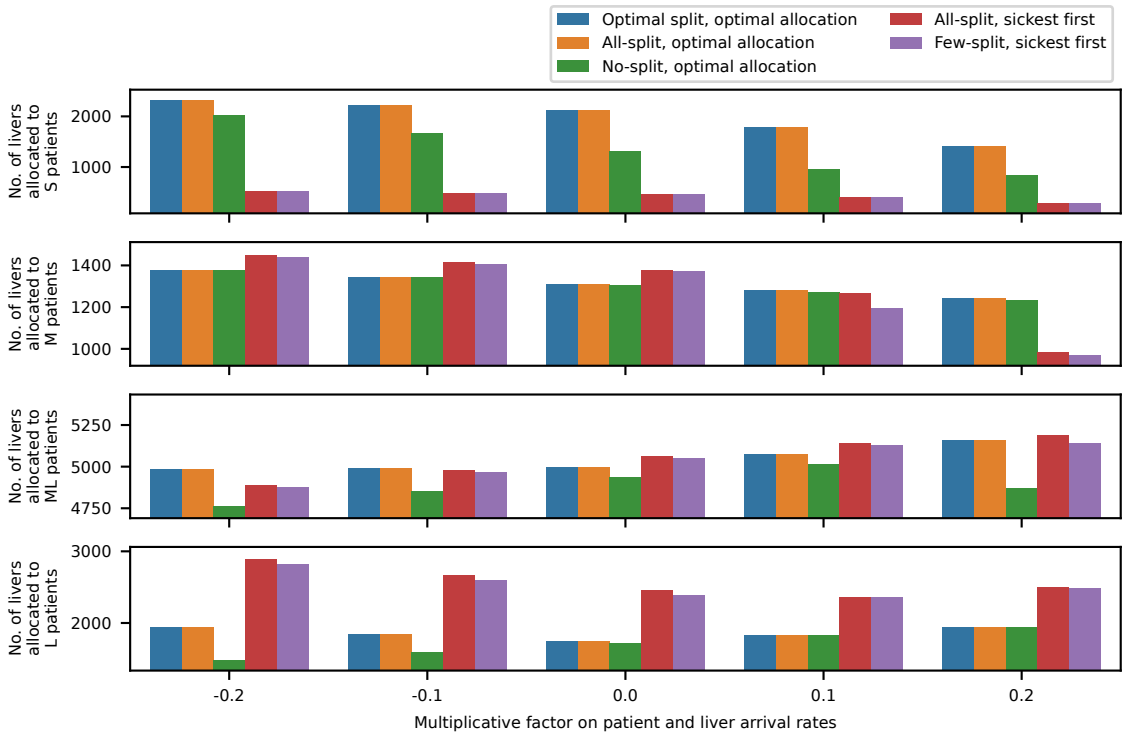

Figure EC.4 **Comparison of allocation decisions under five policies in five simulated settings with different patient and liver arrival rates. This figure demonstrates how varied patient and liver arrival rates affect liver allocation to each patient size group. The setting is the same as in Fig. EC.3.**

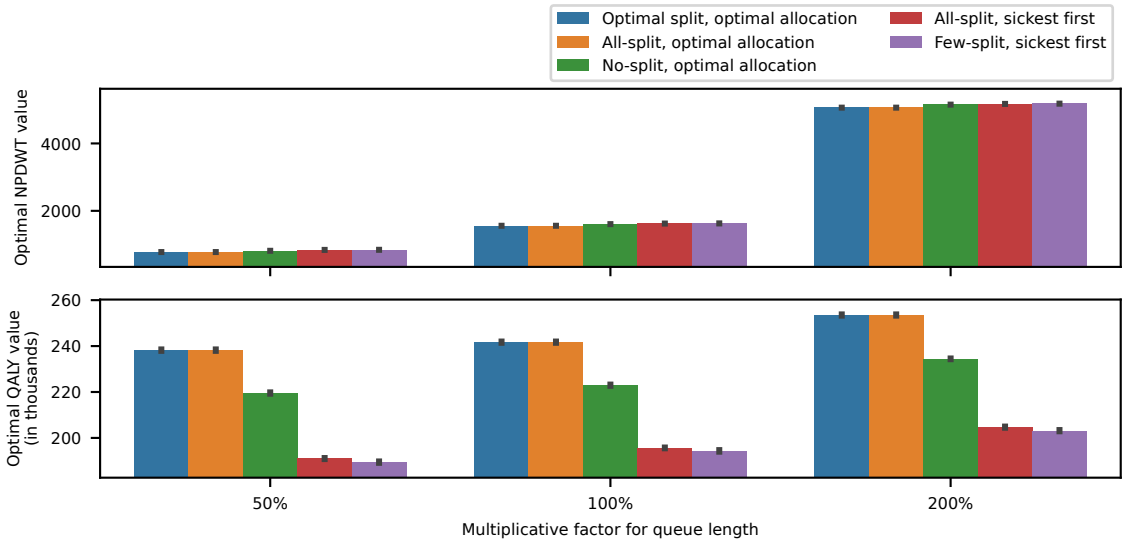

Figure EC.5 **Comparison of five policies in three simulated settings with different initial queue lengths. The initial lengths for all queues are scaled at the same rate.**

large, sicker patients in the opposite direction. Specifically, for the ij-th queue, we multiply its initial length by $100\% + f((i-2.5)/3 + (j-3)/4)$, where f is a multiplicative factor and takes value from $\{50\%, 80\%, 100\%, 120\%, 150\%\}$. For simplicity, here, we number the four size types S, M, ML, and L by $1 \sim 4$; in other words, $\mathcal{I} = \{1,2,3,4\}$. For example, with $f = 80\%$, we multiply the initial lengths of queues $(i=1, j=1)$, $(i=1, j=3)$, $(i=1, j=5)$, and $(i=4, j=5)$ by 80%, 90%, 100%, and 120%, respectively. SLTs robustly improve both objective functions.

Moreover, we examine the effect of liver arrival rates by modifying the liver arrival rates using two approaches. First, we vary the proportions of splittable livers for all liver types between 1% and 30% and we keep the number of livers unchanged (Figure EC.7). Second, we increase the number of splittable livers for one particular liver type by one per day; in other words, $\bar{\mu}^\ell = 0.1\mu^\ell$ for this modified liver type ℓ (Figure EC.8). In addition to the consistent benefits of more SLTs (Figure EC.7, we also note that extra M, ML, and L livers give more marginal benefits than S livers (Figure EC.8).

Lastly, we examine the number of livers allocated to each patient size group to understand how system parameters affect optimal (split) liver allocation decisions. Figure EC.9 shows the numbers of whole and split livers allocated to all four patient size groups in the same five scenarios used in Figure EC.8. The transplantation objective is to maximize QALY. Results show that once again the "optimal split, optimal allocation" policy allocates roughly the same numbers of whole and split livers to all size groups, indicating that "all-split, optimal allocation" remains near-optimal despite parameter changes. Both "optimal split, optimal allocation" and "all-split, optimal allocation"

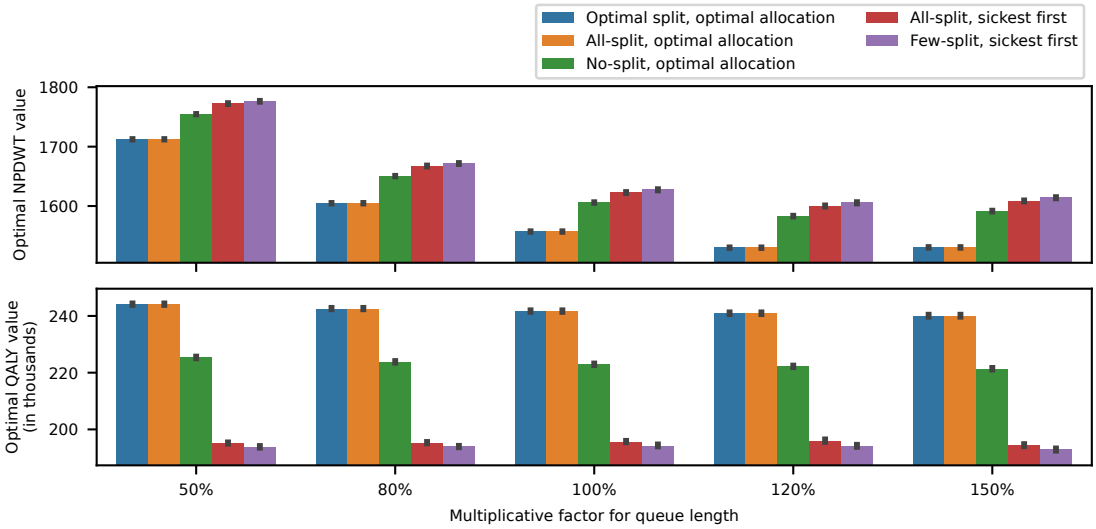

Figure EC.6 **Comparison of five policies in five simulated settings with different initial queue lengths. The initial queue lengths of small, healthy patients and large, sicker patients are adjusted in opposite directions.**

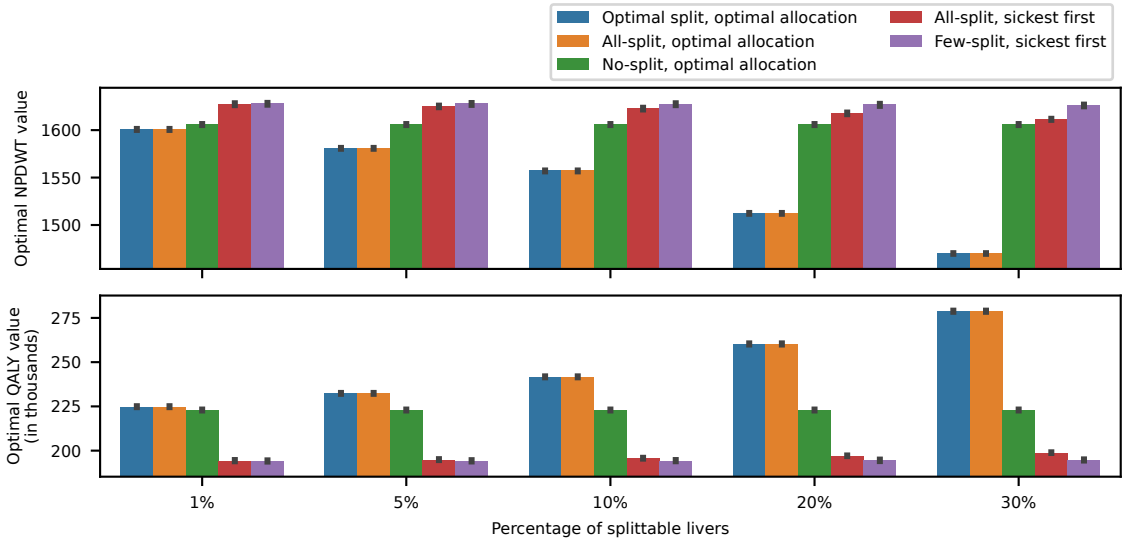

Figure EC.7 **Comparison of five policies in five simulated settings with different percentages of splittable livers. All liver size groups are adjusted at the same rate.**

focus on increasing access for small patients, allocating the greatest number of livers (whole or partial) to size group S compared with other policies. By contrast, "no-split, optimal allocation" assigns far fewer (whole) livers to small patients, suggesting that splitting can significantly boost their access to transplants. Under the two "sickest-first" policies, the number of livers allocated to small patients is the lowest among all policies, whereas the M and L size groups consistently receive more livers. Moreover, any additional livers help increase transplant access: an influx of

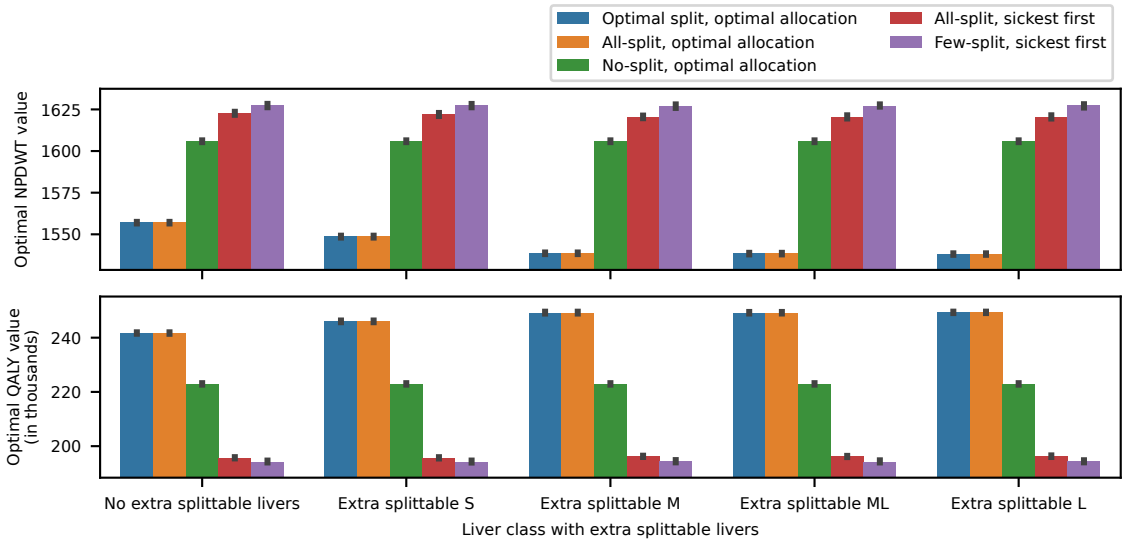

Figure EC.8 **Comparison of five policies in five simulated settings with different percentages of splittable livers. In each adjusted setting, a certain liver size group has an extra splittable liver per day.**

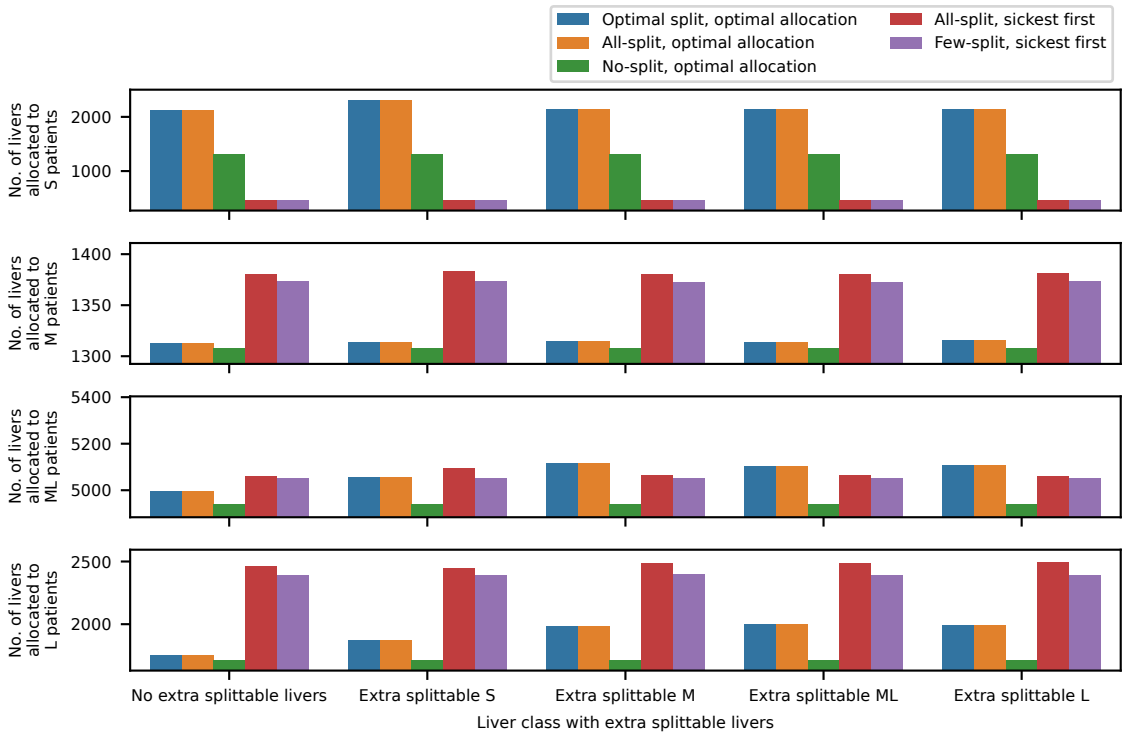

Figure EC.9 **Comparison of allocation decisions under five policies in five simulated settings with different percentages of splittable livers. This figure shows how varying the percentage of splittable livers affects liver allocation across different patient size groups. The setting is the same as in Fig. EC.8.**

smaller livers directly raises the number of transplants for small patients, while additional larger livers can benefit both smaller and larger patient groups through SLT.

EC.11. Future Directions

This paper is the first in its kind that studies fluid models in SLT. We hope to provide insights, recommend policy modifications, generate discussion, and inspire more detailed analyses regarding implementation in the operations research and transplantation communities. For instance, we estimate the SLT outcomes using the data available, but one could do sensitivity analysis regarding outcomes, factoring in selection biases, heterogeneous medical expertise, medical learning, and geographical distributions. For example, Tang et al. (2025) study the donated liver allocation problem in a setting where surgeons with different potential abilities may learn SLT, becoming skilled over time. They formulate a multi-armed bandit that could incorporate first-order queueing dynamics using our fluid limit decomposition.

Reference for the Appendix

Akan M, Alagoz O, Ata B, Erenay FS, Said A (2012) A Broader View of Designing the Liver Allocation System. *Operations Research* 60(4):757–770, ISSN 0030-364X, URL `http://dx.doi.org/10.1287/opre.1120.1064`.

Alagoz O, Maillart LM, Schaefer AJ, Roberts MS (2007a) Choosing among living-donor and cadaveric livers. *Management Science* 53(11):1702–1715.

Alagoz O, Maillart LM, Schaefer AJ, Roberts MS (2007b) Determining the acceptance of cadaveric livers using an implicit model of the waiting list. *Operations Research* 55(1):24–36.

Bertsimas D, Papalexopoulos T, Trichakis N, Wang Y, Hirose R, Vagefi PA (2020) Balancing efficiency and fairness in liver transplant access: tradeoff curves for the assessment of organ distribution policies. *Transplantation* 104(5):981–987.

Bertsimas D, Tsitsiklis JN (1997) *Introduction to linear optimization*, volume 6 (Athena Scientific Belmont, MA).

Boyd S, Boyd SP, Vandenberghe L (2004) *Convex optimization* (Cambridge university press).

Ge J, Perito ER, Bucuvalas J, Gilroy R, Hsu EK, Roberts JP, Lai JC (2020) Split liver transplantation is utilized infrequently and concentrated at few transplant centers in the united states. *American Journal of Transplantation* 20(4):1116–1124.

Kasiske BL, Pyke J, Snyder JJ (2020) Continuous distribution as an organ allocation framework. *Current opinion in organ transplantation* 25(2):115–121.

Marudanayagam R, Shanmugam V, Sandhu B, Gunson BK, Mirza DF, Mayer D, Buckels J, Bramhall SR (2010) Liver retransplantation in adults: a single-centre, 25-year experience. *Hpb* 12(3):217–224.

OPTN, UNOS (2016) Split Versus Whole Liver Transplantation OPTN/UNOS Ethics Committee. Technical report.

Sandıkçı B, Maillart LM, Schaefer AJ, Alagoz O, Roberts MS (2008) Estimating the patient's price of privacy in liver transplantation. *Operations Research* 56(6):1393–1410.

Sandıkçı B, Maillart LM, Schaefer AJ, Roberts MS (2013) Alleviating the patient's price of privacy through a partially observable waiting list. *Management Science* 59(8):1836–1854.

Tang Y, Li A, Scheller-Wolf A, Tayur S (2023) Multi-Armed Bandits with Endogenous Learning and Queueing: An Application to Split Liver Transplantation, URL `https://papers.ssrn.com/sol3/papers.cfm?abstract_id=3855206`.

Tang Y, Li A, Scheller-Wolf A, Tayur S (2025) Multi-armed bandits with endogenous learning curves: An application to split liver transplantation. *Manufacturing & Service Operations Management* .

Tunç S, Sandıkçı B, Tanrıöver B (2022) A simple incentive mechanism to alleviate the burden of organ wastage in transplantation. *Management Science* .

Zenios SA, Chertow GM, Wein LM (2000) Dynamic allocation of kidneys to candidates on the transplant waiting list. *Operations Research* 48(4):549–569.